3-2022

Applying Models of Circadian Stimulus to Explore Ideal Lighting Configurations

Alexander J. Price

APPLYING MODELS OF CIRCADIAN STIMULUS TO EXPLORE IDEAL LIGHTING CONFIGURATIONS

THESIS

Alexander J. Price, Master Sergeant, USAF

AFIT-ENS-MS-22-M-162

DEPARTMENT OF THE AIR FORCE
AIR UNIVERSITY

AIR FORCE INSTITUTE OF TECHNOLOGY

Wright-Patterson Air Force Base, Ohio

AFIT-ENS-MS-22-M-162

APPLYING MODELS OF CIRCADIAN STIMULUS TO EXPLORE IDEAL LIGHTING CONFIGURATIONS

THESIS

Presented to the Faculty

Department of Operational Sciences

Graduate School of Engineering and Management

Air Force Institute of Technology

Air University

Air Education and Training Command

In Partial Fulfillment of the Requirements for the

Degree of Master of Science in Logistics & Supply Chain Management

Alexander J. Price

Master Sergeant, USAF

March 2022

AFIT-ENS-MS-22-M-162

APPLYING MODELS OF CIRCADIAN STIMULUS TO EXPLORE IDEAL LIGHTING CONFIGURATIONS

Alexander J. Price
Master Sergeant, USAF

Committee Membership:

Michael E. Miller, PhD
Advisor

Frank W. Ciarallo, PhD
Co-Advisor

Abstract

Increased levels of time are spent indoors, decreasing human interaction with nature and degrading photoentrainment, the synchronization of circadian rhythms with daylight variation. Military imagery analysts, among other professionals, are required to work in low light level environments to limit power consumption or increase contrast on display screens to improve detail detection. Insufficient exposure to light in these environments results in inadequate photoentrainment which is associated with degraded alertness and negative health effects. Recent research has shown that both the illuminance (i.e., perceived intensity) and wavelength of light affect photoentrainment. Simultaneously, modern lighting technologies have improved our ability to construct lights with desired wavelengths. To improve photoentrainment in low light environments, this research utilizes a multiple regression and multi-objective model to explore the relationship between the wavelength composition of artificial light and circadian stimulus (CS) for a fixed illuminance. The model is used to recommend emitter light intensity and wavelength characteristics that maximize CS in artificial lighting. These results suggest that by carefully choosing the center wavelengths for emitters we can achieve desirable CS values without increasing intensity. In addition, constraining the design to low illuminance values leads to increases in blue wavelength energy and shifts the color of illumination. Finally, constraining the design to a desirable range of colors reduces the size of this effect while still providing desirable levels of CS. The highest CS achieved at 250 lx is 0.669 without consideration for CRI or color difference. Constraining CRI and

color to match D65, the maximum CS at 250 lx is 0.353 with a CRI of 91.1 and a color difference from D65 of 0.0094.

Acknowledgments

I would like to express my sincere appreciation to my faculty advisor, Dr. Michael Miller, for his guidance and support throughout the course of this thesis effort. His knowledge, insight, experience, and patience were integral to the success of this work. I would also like to express my genuine gratitude to my co-advisor, Dr. Frank Ciarallo, who provided knowledge and resources that were essential to this research.

I would also like to express my deepest appreciation to my wife. Her support, sacrifice, and dedication to my thesis and degree completion was essential for our success. I admire her unwavering love, resilience, and motivational spirit that pushes us to be better. Our trials in navigating pandemic parenthood throughout this program are a testament to the profoundness of our teamwork. I hope that our efforts inspire our children to humbly work hard and always seek knowledge and answers that will form their lives for the better.

Last but not least, I express the highest gratitude to my mother, for being a mentor and providing the standards that drive my work ethic and aspirations to achieve.

Alexander J. Price

Table of Contents

Page

List of Figures

Page

List of Tables

Page

List of Equations

Page

APPLYING MODELS OF CIRCADIAN STIMULUS TO EXPLORE IDEAL LIGHTING CONFIGURATIONS

I. Introduction

General Issue

Intelligence, Surveillance, & Reconnaissance (ISR) personnel among others performing sensitive operations are required to work in buildings without natural light. Further, many of these individuals perform shift work, requiring frequent changes in their work schedules. Research has shown that exposure to bright daylight suppress the human body's production of melatonin, a hormone produced to regulate the sleep/wake cycle referred to as the circadian rhythm [10]. Melatonin production reduces alertness and degrades response time which contribute to changes in individuals' levels of performance [27]. Alertness is particularly important in safety critical professions including ISR personnel, first responders, healthcare providers, pilots/aircrew, and air traffic controllers among others. These services must be delivered on a continuing basis, leading to long working hours. Management of these services includes creating shift work schedules, which requires attention to natural human sleep rhythms. In many cases, sleep and wake schedules for a particular worker may be irregular, changing from day to day.

Research has also shown that some wavelengths of light are particularly useful for suppressing melatonin, especially in dim lighting environments [12]. Employment of these wavelengths in work environments could be useful for maintaining alertness and supporting acceptable response times. The wavelengths that suppress the body's

production of melatonin are found in most lighting fixtures, sunlight, and device screens. The human body produces more melatonin in dim or low light conditions resulting in increased sleepiness and decreased alertness [11]. Dim or no light is also the regulatory state of lighting for certain ISR work spaces, such as imagery analysts, where low light conditions enhance the visibility of low contrast objects on electronic displays.

Problem Statement

The relationship between short wavelengths of illumination and melatonin suppression has been studied in many different ways. Recently researchers have attempted to construct a model to quantitatively predict how different lights effect the circadian system. These models predict the spectral sensitivity of the human circadian system with a circadian stimulus (CS) metric. One such model created by the Lighting Research Center (LRC) [20] permits the circadian stimulus of light to be predicted based upon prior studies. Results from these studies allow the computation of the circadian stimulus as it varies from threshold to saturation based on numerical representations of the human eye's sensitivity to input wavelengths of light. This permits the prediction of melatonin suppression or production in individuals exposed to illumination of different spectral composition and intensity. The optimal spectral composition derived from this model can be used to design illumination requiring the least illuminance to achieve a desired level of melatonin suppression. Allowing lights to be produced which are lower in perceived brightness or require less electrical power while producing an increased level of melatonin suppression would be beneficial. However, current work place standards often do not consider this factor but mandate low ambient light levels to

enhance display contrast and aid object detection within displayed images. Therefore, they often do not adequately consider the effects of the low-level lighting conditions on the natural circadian rhythm and alertness. Using the LRC model, Figure 1 provides a generic visual of the spectra generated by common lighting sources and their corresponding circadian values of light and stimulus.

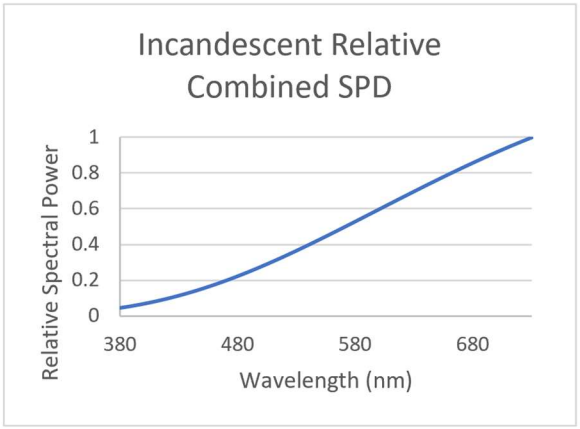

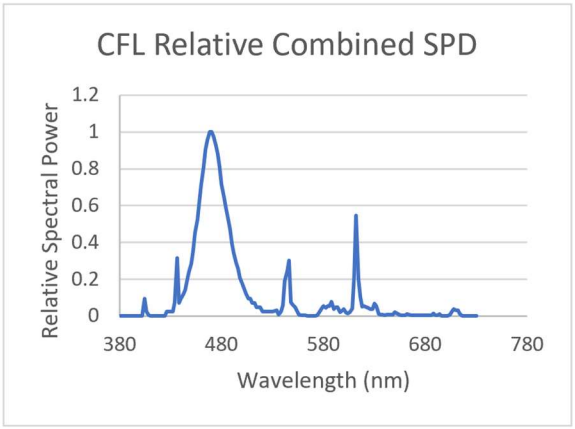

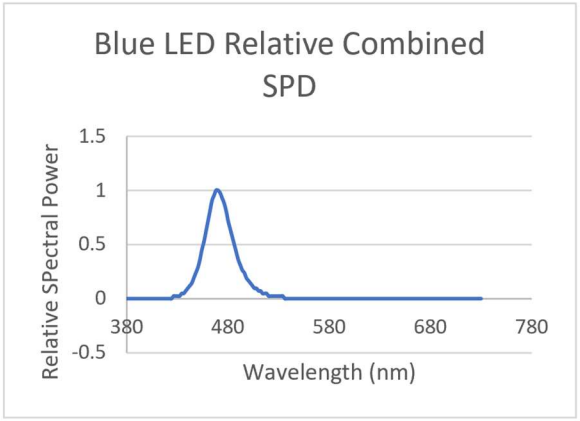

Standard Incandescent 450lx	Combined Illuminance (lux)	450
	Circadian Light (Cla)	449.9613216
	Circadian Stimulus (CS)	0.395106452
GE CFL FLE15TBX L LLCD 2700K 450lx	Combined Illuminance (lux)	450
	Circadian Light (Cla)	310.7066234
	Circadian Stimulus (CS)	0.323953291
Blue LED 450lx	Combined Illuminance (lux)	450
	Circadian Light (Cla)	7843.306718
	Circadian Stimulus (CS)	0.677626166

Figure 1: Standard Lighting Spectra [30]. SPD: Spectral power distribution

The need for dim to no light in workplaces which require critical analysis of images on electronic displays arose from the issue of glare. As ambient light is reflected from these displays the contrast of objects on the display is reduced which can affect the

human's ability to accurately interpret the displayed imagery. The ISR community in particular currently requires very low ambient illumination levels. Glare on screens has improved greatly over time with device screen technology but still compromises detail detection, which cannot be tolerated when detail is critical. The low levels of ambient illuminance are intended to reduce the light that reflects off the display screens to increase contrast and increase accuracy of interpreting visual information [29]. Requiring low illuminance levels decreases the amount of short wavelength light exposure personnel receive working in these environments. This reduces the circadian stimulus and impact's the human body's ability to establish a strong circadian cycle. The sun in natural environments provides the establishment of a strong circadian cycle.

Research Hypothesis/Focus/Questions

This research is focused on the non-visual effects of light exposure. Utilizing models of circadian stimulus, this research investigates the optimal wavelengths of light that improve human circadian rhythms while meeting other lighting requirements within particular environments. This research investigates the use of modern lighting technology to construct desired wavelengths of light. Furthermore, it determines optimal spectral light composition at a fixed illuminance. Finally, this research recommends the intensity of light as a function of wavelength to yield an optimal circadian stimulus.

Hypothesis

The spectral composition of light can be manipulated to achieve desired CS values with minimum luminance. Considering the evidence of circadian rhythm sleep disorders and related physical and mental health issues, the Air Force should explore the effects of simulated natural lighting on the ISR community, decision makers, and shift working personnel across the DoD. Improved lighting which achieves desired CS values with a reduced perceived brightness will enable: (1) effective task performance for human operators across the DoD community, (2) improved mental and physical health for these operators.

Research Focus

This research utilizes non-linear mathematical models, multiple regression analyses, and a genetic algorithm to generate a pareto front. The optimal spectrum provided by artificial lighting is the design that best enables analysts to maintain the same or improved ability to detect detail on device screens (or that meets existing light level requirements), while receiving a higher CS than is possible with current lighting practices. Note that there is significant focus on modern lighting systems which possess tunable lighting spectra which has not been possible with previously available technologies. Modern technologies include the addition of phosphors or quantum dots to emitters, such as light emitting diodes (LED's), to convert short wavelength light to longer wavelength light and create different perceived colors. The research described in this thesis focuses on identifying specifications for spectrally optimized LEDs.

Investigative Questions

Q1: Can a lighting spectrum be crafted from a number of emitters that increases CS at a constant illuminance?

Q2: Is this increase in CS significant in contrast to a reference light, i.e., typical D65 LED or fluorescent lighting?

Q3: Can variables such as color rendering index (CRI) or color distance from a reference light be traded for increases in CS?

Methodology

This research uses mathematical models to generate parameterized spectra. The primary focus of this research uses existing models of circadian stimulus, specifically a model created by the LRC. This model permits CS to be estimated as a function of the intensity of light at different wavelengths. In addition to their impact on CS, intensity and wavelength also affect the color temperature and visual efficacy of light. Thus, this research is novel in that it considers the effect of the spectral composition of illumination on CS as well as the color and efficacy of the illumination.

The model calculates Circadian Light Intensity (CL_A) as discussed by Rea & Figeiro [31]. This model requires inputs which include the spectrum of light that hits the human eye, the illuminance at the human eye, correlated color temperature (CCT) of illumination, and the melanopsin lens data as developed by Rea & Figeiro [31]. The output is the CL_A value. An additional model converts CLA to CS values. The current research embeds this function within a MATLAB construct which permits calculation of

CS as a function of illuminance value and changes in the wavelength composition of light within a wavelength range of 380nm to 620nm. The model can be constrained based upon the color of illumination.

This model is applied in a three-phase analysis. Phase I is accomplished by creating MATLAB functions in the Gaussian models to determine what parameters are necessary or useful. This analysis determines the multivariate space required to produce the outcome of CL_A and CS. Phase I also determines the variables that will be used to assess the trade-offs of color, relative efficiency, and CL_A and CS in Phase II & III. Since higher CS values can be obtained by increasing luminance or changing the wavelength of light, Phase II focuses on a multiple regression analysis of the variables that illustrates these spaces and relationships. Phase III uses a genetic algorithm optimization to generate a pareto front that allows in depth analyses of the trade-off associated between color and CS.

Assumptions/Limitations

Although there are therapeutic settings where the non-visual effects of light are more closely considered, residential and facility lighting is typically designed for light to cover the largest area at the lowest cost. This highlights a limitation of current practices since work and home are where most individuals spend the majority of their time. Therefore, it is productive to focus on one or both of these settings. We assume that CS equations accurately predict the influence of illumination on human circadian systems. We then assume that resulting illumination must comply with specifications with respect to a reference light and low luminance, while incorporating acceptable quality in terms of

efficacy and color quality. Finally, we assume that these lamps can be effectively produced which have the spectra produced by the optimization.

This research explores improvements enabled by modern lighting technologies utilizing the information regarding non-visual effects of light. Therefore, this research is limited in that constraining the model to low illuminance values requires increases in blue wavelength energy and shifts the color of illumination. Further constraining the model to a range of colors reduces the size of this effect but provides an increased control of the circadian stimulus.

Implications

With appropriate models to support the design of work environments, the DoD can leverage lighting technologies to improve mission performance and prevent military and civilian members mental and physical health issues related to circadian rhythm disruption via improper artificial lighting.

II. Literature Review

Chapter Overview

The following review summarizes the existing research on the influence of light on human circadian rhythms. Issues explored include how the characteristics of lighting effect human circadian systems. In addition, this section summarizes research on how exposure to lighting influences human performance. To address this more specifically, we reexamine current lighting standards which are based only upon the impact of workplace illumination on visibility and comfort. This literature review seeks to expand the considerations of lighting to include its impact on human circadian response. This chapter will summarize knowledge of the background research in this area from different perspectives to provide the reader with an understanding of the framework of the proposed research and refine the scope of the problem. Finally, this literature review will conclude by summarizing gaps in research and a discussion of how workplace lighting standards might be adapted as a result of this empirical study.

Definitions

To understand this research, it is important to define technical terms and practices. These provide a necessary understanding of the human eye and the functions of the retina for communicating light exposure to the brain. In particular, this information represents how light exposure affects the physiological and chemical responses that relate to sleep/wake cycles. Further, it is important to utilize metrics relating to measuring light effects on human circadian systems. These metrics can be complicated to define and

calculate. They provide the necessary quantitative information that allows precise conclusions to be drawn in this research.

Circadian Rhythms

A circadian rhythm is the body's internal 24-hour clock that regulates falling asleep and waking up. This is also known as the sleep/wake cycle, it is naturally aligned with the rising and setting of the sun. Some of its impacts include, changes in body temperature, metabolic activity, and hormone response [16]. Since the invention of artificial light, this cycle's alignment with natural light is often disrupted. Before artificial light was invented the lighting component of human circadian rhythm came from the natural lighting produced during the day and removed at night. As the sun rises, crosses the sky, and sets, light on the earth changes both in intensity and the relative intensity across the wavelengths in the visible spectra. Different wavelengths of light trigger different physiological responses in the body signaling it to be alert, or wind down for rest and regeneration.

Anatomy of the Human Eye

The basic anatomy of the human eye includes the lens, iris, cornea, ciliary muscle, sclera, extraocular muscles, retina, and optic nerve. The retina and what happens within the retina is of specific importance when considering the non-visual effects of light. It is comprised of three layers; the back layer is the photoreceptor that is responsible for translating light to the brain called rods and cones [9]. The ganglion cell and bipolar cell layer are located on top of the photoreceptive layer. These cells collect

signals from multiple rods and cones, synthesize these signals and provide the synthesized signal to the brain via the optic nerve. Rods handle vision that deals with low light levels which does not include color vision or spatial acuity. Cones compliment the rods by receiving high light levels to deliver high spatial acuity and color vision. S-cones, M-cones, and L-cones are the three types of cones. Where the first letter of each stand for short, medium, and long wavelengths respectively roughly corresponding to the wavelengths of light that we refer to as blue, green, and red [7], [8].

Artificial Light vs Natural Light

Unlike natural light, artificial light does not contain the full spectrum of colors. For this reason, natural light is more desirable for positive mental health outcomes [1]. Natural light changes color with the suns angle, while artificial light typically has a constant color. Another important difference is that artificial light can be present when there is no sunlight at night while asleep. When driven by natural light, the body's core temperature decreases at night and increases during the day as part of the circadian rhythm sleep/wake cycle. A 1991 study observed no body core temperature changes in participants subjected to dim lights at night, and a significant increase in body core temperature in participants subjected to bright lights at night. This resulted in modified sleep cycles, ultimately negatively impacting sleep [12].

Modern Lighting Technologies

Modern lighting systems have tunable lighting spectra leveraging technologies that were not previously available. Phosphors and quantum dots can be

added to emitters, such as light emitting diodes (LED's), to convert short wavelength light to longer wavelength light and create different perceived colors.

Intrinsically Photosensitive Retinal Ganglion Cells (ipRGCs)

Between 1990 and the early 2000's a number of studies discovered what are called intrinsically photosensitive retinal ganglion cells (ipRGCs). While light was known to affect the body's circadian response prior to this discovery, the mechanism for this effect was unknown. These ipRGCs are among the retinal ganglion cells and constitute a very small proportion of the retinal ganglion cells represented in Figure 2. This small proportion of newly discovered retinal ganglion cells are now believed to play a significant role in regulating the non-visual effects of light. We now know that ipRGCs are responsible for responding to and regulating the way the brain processes light and dark to regulate the circadian rhythm [13]. Where circadian optimization is the primary objective, understanding the response of the ipRGCs is essential.

The intrinsically photosensitive retinal ganglion cells (ipRGCs) are responsible for relaying these signals based upon light to portions of the brain that do not contribute to vision but influence our internal clocks and perception of time of the day. The ipRGCs translate signals corresponding to light irradiance through the optic nerve to the superchiasmatic nucleus (SCN) as shown in Figure 3, which is a small cluster of cells located in the front of the hypothalamus. The reaction influences multiple functions, but broadly influences photoentrainment of the circadian rhythm [22].

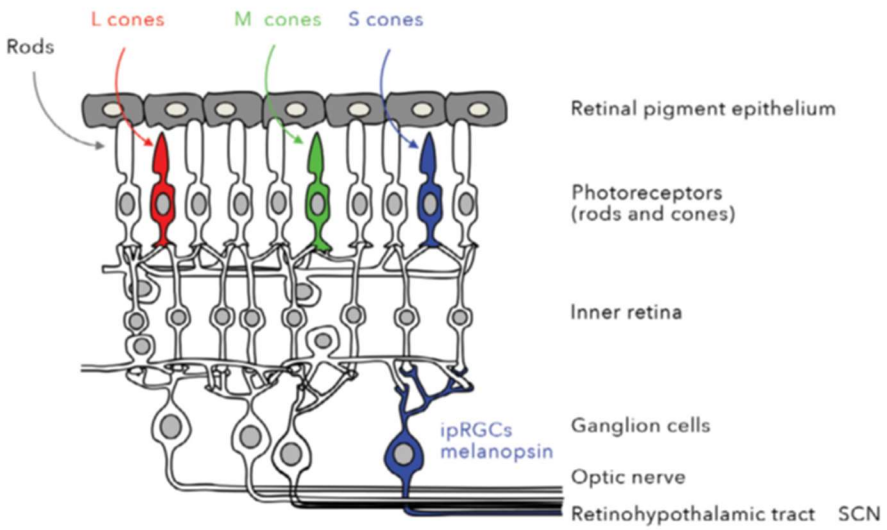

Figure 2: Schematic of Human Retina [14]

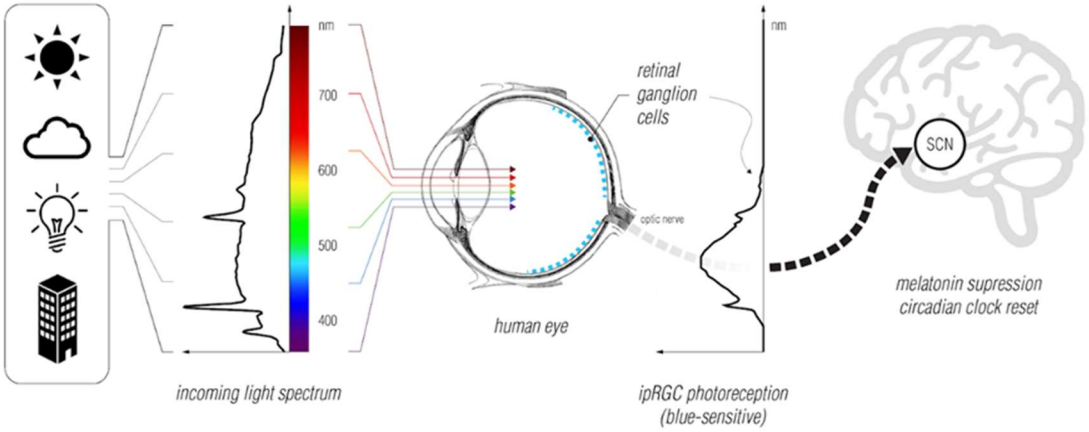

Figure 3: Path to superchiasmatic nucleus [25]

Melatonin & Sleep/Alertness

Melatonin is the neurotransmitter that reduces alertness and promotes sleepiness. When the human retina is exposed to light having sufficient intensity at appropriate wavelengths, the electrical signals transmitted to the SCN can suppress the body's production of melatonin, thus reducing the promotion of sleep. The ipRGCs are sensitive to blue wavelengths corresponding to blue light. Exposure of the visual system to these wavelengths is particularly useful in suppressing physiological responses needed to produce melatonin and promote sleep. The theory of sleep debt speculates that this exposure to melatonin suppressing wavelengths of light that inhibit sleep is a compounding event that effects overall health and performance. The ipRGC's photosensitivity allows them to respond to the intensity of short wavelengths of light and inform the brain that it is either time to produce melatonin and rest, or suppress melatonin and remain alert [14]. However, it is possible to elicit alertness with red light without suppressing melatonin [20].

Photoentrainment

We know that light controls our circadian systems 24-hour sleep-wake cycle. The process of how the human rhythm adjusts in response to natural and artificial light is known as photoentrainment. The physiological responses associated with photoentrainment include changes in body temperature and heart rate. The photoentrainment process begins based on messages received from the ipRGCs in response to the light which they and other sensors in the eye receive [10]. The process of

photoentrainment and the influence of the ipRGCs are important to the optimization models in Section III.

Vision & Wavelengths of Light

The wavelength of light is measured using nanometers (nm) and has a visible range of approximately 400-700 nm. A difference in the relative intensity of energy at different wavelengths translates to a difference in color to the human eye. The intensity of light at each wavelength is typically measured in Watts or Joules. The primary colors are blue, green, amber, and red (in increasing order of wavelength). These colors can be created by utilizing narrow bandwidth emitters. However, most colors of light are comprised of multiple wavelengths of light which are interspersed across the visible spectrum [26].

Relevant Research

Bolton [5] uses Electroencephalography (EEG) and Electrooculography (EOG) on subjects while exposed to blue and white light and administering six cognitive tests measuring cognitive effects of these wavelengths. The study concluded that a bluish white and blue light had similar results on the participants' initial alertness, but differed in two areas. White light proved to increase test results in tasks requiring a choice decision, and also proved to maintain alertness longer than blue light. This was determined based on the results of the Stanford Sleepiness Scale showing a slower decline in alertness with white light than blue once the bright light was removed, summarized in Table 1.

Miller [4] focuses on intelligence, surveillance, and reconnaissance (ISR) imagery analysts, the dim lighting conditions they work in, the lighting specifications of electronic displays, and overall built environment they work in. Using low contrast Gabor patches on a display, subjects were exposed to four different levels of ambient light arranged in different orientations. Their response time to changes in intensity of the Gabor patches was used as an indicator of performance level. They also monitored alertness and discomfort. Results showed a significant relationship between the orientation of the light and sleepiness, weariness, and discomfort. Overall, this study showed a significant increase in performance with higher levels of illumination.

Mental health and the built environment have been an area of increasing focus for research and experimentation with findings in support of the connection between the two. The workplace and residence are where we spend most of our time and the 2020 pandemic has increased time individuals spend in their residences. Kohl [1] focuses on the lighting of the built environment and the mental health of its occupants, using different measures to assess the effects of lighting. The data was obtained through mental health questionnaires and a survey to determine the lighting situation of each participants-built environment. The results showed a relationship between natural light and mental health. More natural light indicated a higher level of mental health, and inversely emotional well-being and health decreased as natural light decreased.

As of 13 may 2021 there are no specific regulations in lighting that consider the non-visual effects of light on humans. Since spectral sensitivity of visible brightness and non-visual effects differ, Stefani and Cajochen [21] recommends considering Melanopic equivalent daylight illuminance (melEDI) per Watt along with Lumens per Watt as a

measure of luminous efficacy. MelEDI is a suitable measure for predicting non-visual effects in humans but can be difficult to identify a specific quantity to elicit the effects of the output in question (i.e., alertness, sleepiness, etc.). Figueiro, et al [20] studies lighting to elicit Circadian Stimulus (CS) values ≥ 0.3 meaning alertness would increase and sleepiness would decrease at a significant level if $CS \geq 0.3$. The experiment gathered baseline photometric spectrometer data via analyses of existing lighting to ensure the lighting changes used for the study would be sufficient to produce values of $CS \geq 0.3$. Using 94 participants across 4 sites, values of $CS \geq 0.3$ during daytime hours were associated with an acute alerting effect on office workers across all four locations. Sleepiness was determined with KSS.

Miller et al, [27] uses two optimization models upon which this research will expand. Lighting updates and developments in solid-state lighting sources have allowed more versatility in accurately controlling narrow-band emissions by tuning them while requiring low voltage sources. Using this technology, they built an independent light source and co-optimization model that are constructed to optimize the location of a 30 and 60 nm bandwidth narrow-band emitters. The correlated color temperature (CCT) of the illumination was controlled by changing the varying light sources relative intensity. Results indicated that without constraints, at least 3 emitters were able to produce a lamp with high color rendering index (CRI) values with reference to daylight illumination across CCT values between 4000 K-10,000 K. Applying parameters mandating emitters be the same in both light sources resulted in a minimum of four 30 and 60nm bandwidth emitters.

In the research summarized below, light is measured in a way that relates to color and intensity. The other primary measurement sought is some form of performance metric (i.e., sleepiness, alertness, reaction time etc.,). Some physiological measurements such as melatonin or vitamin D levels, as well as electroencephalography (EEG), and electrooculography (EOG) are also used in related research. Light is typically used as the independent variable, and the performance or physiological response of those exposed to the lights is the dependent variable. The following segments include the highlights of independent and dependent variables. A brief summary of the effects and results from interested studies is provided below.

Table 1: Summary of inputs and outputs from Bolton's research

<table>
<tr><th colspan="2">Bolton [5] n = 16</th></tr>
<tr><th>Inputs</th><th>Outputs</th></tr>
<tr><td>460nm Blue light at 200lx</td><td>Response time</td></tr>
<tr><td>D65 White light at 200 lx</td><td>Response control</td></tr>
<tr><td rowspan="5">Participants exposed for duration of 30 minutes at 200 lx then reduced to 3.5 lx while cognitive tests were administered</td><td>Selective attention</td></tr>
<tr><td>Working memory</td></tr>
<tr><td>Semantic memory</td></tr>
<tr><td>Stanford Sleepiness Scale</td></tr>
<tr><td>Measured using EEG & EOG equipment</td></tr>
</table>

Bolton Thesis $n = 16$

Independent Variables: x_1=460nm blue light f/30 min, x_2=D65 white light f/30 min (both of 200 lx) After 30 minutes of exposure to either of these two options, the light was reduced to 3.5 lx of D65 light while six cognitive tests were administered, the results of which would constitute as the dependent variables below.

Dependent Variables: y_1=response time, y_2=response control, y_3=selective attention, y_4=working memory, y_5=semantic memory, y_6=Stanford Sleepiness Scale. EEG and EOG equipment were used to help read frequencies associated with how awake participants are, along with rate of slow eye movements and eye blinks.

Results/Effects: Research seeks to understand the relationship between blue light and cognitive performance. Results of tasks requiring decision making were better after the white light exposure than under the blue. The sleepiness scale results showed that alertness decreased at a slower rate after D65 white light than blue. Accuracy results were similar between both lights.

Rensselaer Polytechnic Institute Lighting Research Center; Figueiro, et al

Independent Variables: x_1=Desktop Luminaires, x_2=Overhead Luminaires, x_3=Desktop & Overhead Luminaires Lighting set at Circadian Stimulus (CS) values $\geq$0.3. CS Values determined by Daysimeter. Two days of intervention where these lights were directed at participants eyes. These lights exposed participants to more daylight wavelengths than they would normally experience.

Dependent Variables: Of the office workers while at work. y_1= Sleepiness, y_2= Alertness, y_3= Vitality, y_4= Energy.

Results/Effects: Light monitoring was used in advance to determine baselines of worker exposure, as well as the difference in the values of the exposure during interventions. Other actions taken were questionnaires about workers sleep habits, stress, and subjective feelings of the dependent variables. Results showed significant reductions in sleepiness levels during intervention days. Significant results reporting feeling more

vital, energetic, and alert. Ultimately determining that lighting producing "$CS \geq 0.3$ can reduce sleepiness and increase vitality and alertness in office workers" [20].

Note: High light levels are classified as being $CS \geq 0.3$ and low light levels as $CS \leq 0.15$.

Table 2: Figueiro, et al experimental depiction

Inputs	Outputs	Control
Desktop luminaires	Sleepiness	Light monitor
Overhead luminaires	Alertness	Used to measure typical wavelength exposure of participants outside of treatment
Desktop & overhead luminaires	Vitality	
Lighting treatment for two days with CS ≥ 0.3	Energy	

Metrics

This section will provide an explanation of the quantitative methods used and referenced throughout this research.

Luminance: Luminance, (L_v) measures the perceived brightness of an object. L_v can vary with different wavelengths of light. This metric is particularly important since it will allow us to determine which lights with differing spectra are perceived as brighter [26].

$$\boldsymbol{L_v = k_m \sum_{\lambda=380}^{760} \big(s(\lambda) V(\lambda)\big)}$$

Equation 1: Luminance

Correlated Color Temperature (CCT): CCT is commonly referred to on a warmth to coldness scale, or as tone and is represented in units of Kelvin. Natural

daylight color temperatures have a range of approximately 3700-35000K during a typical day. The color of emission closely matches the color of a light with the same color temperature. This can be mathematically defined by a perpendicular line to the Planckian locus which intersects the point defined by the 1931 CIE diagram coordinates of the specified light. The color temperature of the light through which this line passes is the CCT [26].

Color Rendering Index (CRI): CRI, denoted as R_a, measures the quality of an artificial light source. CRI uses a natural light source as a reference. A low CRI indicates that the color of artificial light leads to illuminated objects that may be perceived as unnatural. Alternatively, a high CRI indicates that the color of objects illuminated by artificial light compare well with the reference illumination [26].

$$\boldsymbol{R_a = 100 - \frac{4.6}{k}\sum_{i=1}^{k} d_i}$$

Equation 2: Color Rendering Index

Circadian Stimulus (CS) values: The Lighting Research Center (LRC) at the Rensselaer Polytechnic Institute created a metric that quantifies the effects that light has on the human circadian system referred to as circadian stimulus (CS). CS specifies the light source in terms of its intensity and spectrum. CS determines the effects light has on the human circadian system by how much it suppresses melatonin. The level at which the body suppresses melatonin is a significant indication of the body's interpretation of the time of day. The range of CS values are 0.1 to 0.7. A low threshold of 0.1 represents no measurable amount of melatonin suppression; and a saturation of 0.7 represents the

maximum observable melatonin suppression. The LRC recommends that CS should not be determined solely on CCT. Since manufacturers specifications are not equal, neither are the spectral compositions of the light. Melanopic lx, which represents the integrated light received by the ipRGCs based upon their spectral sensitivity, is also not a recommended metric since it only considers the ipRGC's and not the other rods, cones, and RGC-s [22, 24].

To obtain the CS values, two functions are required. The first function is shown in Equation (4) and determines CL_A which represents the specified spectral irradiance that hits the eye. This function is analogous to the $V\lambda$ (Photopic Sensitivity Function) and $V'\lambda$ (Scotopic Sensitivity Function) which quantify the effects of illumination based upon visual sensitivity. The components of CL_A are computed in Equation (4) by multiplying the energy of a light source at each wavelength by the eye's sensitivity to that wavelength of light and integrating the result (i.e., summing digital values) across all wavelengths. This measure reflects the spectral sensitivity of the circadian system. The second function is shown in Equation (3). It computes CS as a function of CL_A, reflecting the absolute sensitivity of the circadian system. CS values thus quantify melatonin suppression as a function of the amount and wavelength of light [22].

$$CS = 0.7 - \frac{0.7}{1 + \left(\frac{CL_A}{355.7}\right)^{1.1026}}$$

Equation 3: Circadian Stimulus

$$CL_A = \begin{cases} 1548\left[\int Mc_\lambda E_\lambda d\lambda + \left(a_{b-y}\left(\int \frac{S_\lambda}{mp_\lambda} E_\lambda d\lambda - k\int \frac{V_\lambda}{mp_\lambda} E_\lambda d\lambda\right) - a_{rod}\left(1 - e^{\frac{-\int V'_\lambda E_\lambda d\lambda}{RodSat}}\right)\right)\right] \\ if \int \frac{S_\lambda}{mp_\lambda} E_\lambda d\lambda - k\int \frac{V_\lambda}{mp_\lambda} E_\lambda d\lambda > 0 \\ 1548\int Mc_\lambda E_\lambda d\lambda \; if \int \frac{S_\lambda}{mp_\lambda} E_\lambda d\lambda - k\int \frac{V_\lambda}{mp_\lambda} E_\lambda d\lambda \leq 0 \end{cases}$$

Equation 4: Circadian Light

Equation (3) shows how CS values are calculated and Equation (4) details how CL_A is determined.

Research Gaps

The results of Figueiro, et al [20], utilizing the CS values previously mentioned expresses the need to reexamine the current lighting standards. It is important to note that the CS value seems to be a loose metric in terms of accuracy. However, it is sufficient in determining significance of short wavelengths and alertness. The study mentions that a more accurate metric may be necessary for measuring the same significance with redder longer wavelengths of lights to cause alertness while avoiding melatonin suppression [20]. Their study does not investigate the impacts of history and duration of lighting interventions on daytime sleepiness and energy levels, but mentions that further research is needed [20].

Summary

The importance of this research on the non-visual effects of light is increasingly valuable considering the evidence of positive and negative results to sleepiness, alertness, health, and workplace productivity based on exposure. This exposure at times that are not synchronous with the sun's cycle can have negative impacts on health and performance. The scope of this research will encompass an optimization model utilizing advanced options in mathematical modeling of variable light controls to achieve uniform color rendering index followed by a reexamination of workplace lighting standards with the non-visual effects considered.

III. Methodology

Chapter Overview

This chapter will describe the techniques and tools used to determine the spectral content to obtain optimal CS values. The methodology involves modeling lamps with different spectral content to assess its impact on metrics, including CS. The results which involve selecting spectral content to maximize CS for a given illumination level can be leveraged to design lamps which promote enhanced circadian rhythms for workers in dim workspaces.

Table 3: Phases of Methodology Diagram

Emitter Pair Selection	
Inputs	**Outputs**
Blue wavelength peaks	All pairs that intersect D65
Yellow wavelenght peaks	
Blue bandwidths	
Yellow bandwidths	

Regression Model	
Inputs	**Outputs**
Blue center wavelength	Circadian Stimulus (CS)
Blue bandwidth	
Yellow center wavelength	
Yellow bandwidth	
Luminance Ratio	

Genetic Algorithm	
Inputs	**Outputs**
Emitter 1 wavelength center	CS
Emitter 1 bandwidth	CRI
Emitter 2 wavelength center	Color Difference
Emitter 2 bandwidth	Relative Efficacy
Intensity of illumination (lx)	Ratio of luminous intensity between emitters

Much of the analysis will assume that illuminance will remain constant at 21.5 lx or 250 lx according to the National Center for Geospatial Intelligence Standards (NGA). These standards mandate that illuminance must be ≤ 2-foot candles which converts to 21.5 lx [28]. The wavelength, bandwidth and luminance of each of two emitters will vary

to represent changes in spectral content produced by the combination of emitters. Additional inputs will be discussed in detail, but the primary data analysis methods performed in this work consist of regression analysis and genetic algorithm with pareto front for multi-objective optimization. The variables of measurement for the non-linear model and regression analysis are as follows:

Regression Variables

The independent variables describe characteristics of the emitters. The dependent variable is the circadian stimulus, as computed from Equation (3).

Independent Variables

1. Illuminance held constant at either 21.5 lx or 250 lx
2. Number of emitters (a constant 2 in this case which renders this a control variable)
3. Peak wavelengths nm
4. Wavelength bandwidths nm
5. Luminous Intensity Ratio of Emitters (denoted as m2)

Table 4: Regression Variables

Independent Variables	Dependent Variable
Illuminance	Circadian Stimulus
Number of Emitters	
Peak Wavelengths (nm)	
Wavelength Bandwidths (nm)	
Luminous Intensity Ratio of Emitters	

Formulas & Methods

Measuring Light

Illuminance represents the amount of light that directly falls upon a surface regardless of whether it is from the emitter source or reflected from another surface. Luminance is the light that is emitted by a surface [26]. These definitions help clarify the reflective and emissive character of light which is critical to how light characteristics relate to human performance in this research. The following details of light measurement provide additional information to aid in the understanding of the photometry/colorimetry relevant to this work. Measurements of light begin with the base unit called a candela, which is defined as the amount of light emitted by a standard candle. One candela from a single source of light emits one lumen per solid-angle (steradian) in every direction, also referred to as isotropic emission [15]. Luminance is the spectrum of visible light emitted from a single source and is measured in lx, equal to lumens per meter squared [15].

Methods for measuring light focus on specific wavelengths of light in the visible electromagnetic spectrum. The visible spectrum ranges from 400-700 nanometers (nm) generally [18]. We chose to perform measurements and optimization primarily using MATLAB functions based on calculations consistent with acceptable SI units. The exception to this is the LRC's non-linear model representing CLA and CS. The Commission on International Education (CIE) developed the CIE 1931 color space used in this work to define the relevant properties of light mathematically. Although research continues to grow and change regarding circadian lighting metrics, the LRC's CS model

was chosen as the primary dependent measure as it is available and based upon reasonable scientific evidence.

An appropriate definition of the color space based on radiance and luminance is central to the representation of light in this research. This is particularly important to light's perceived brightness. The curve shown in Figure 4 is the photopic sensitivity function denoted as Vλ, which illustrates the sensitivity of the eyes during daylight conditions. Note that this curve is based on the average human sensitivity of the three cones' collective responses. Understanding the Vλ function supports understanding the computation of luminance. If we recall Equation (1) in Chapter II, we multiply the radiance (Sλ) in units of watts by the sensitivity function (Vλ) at each wavelength and then sum this across all wavelengths in the visible spectrum. A constant $K_m = 683.002$ lumens per watt is then used to normalize this sum. Although luminance determines which of multiple lights having different spectra will be perceived as brighter, luminance values do not have a linear relationship with perceived brightness. The relationship between luminance and perceived brightness is more accurately defined as a logarithmic response [26].

To begin an explanation of the chromaticity space, the model utilizes a representation of the relative sensitivity of the three cones of the human eye that vision relies upon. This enables a direct calculation of a number of useful metrics based on these three relative sensitivity values. The CIE 1931 color space model allows a simple representation of spectral data based on colors perceived by the human eye using these three cone representative figures, called tristimulus values (XYZ).

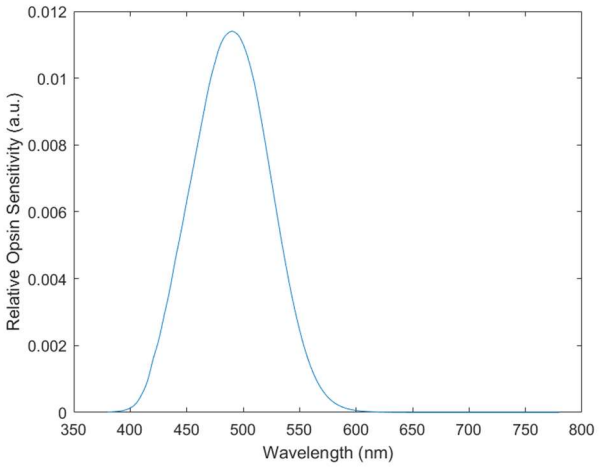

Figure 4: Vλ Peak Opsin Sensitivity function (MATLAB)

The method used in this research to transform spectral energy to the CIE color space will apply tristimulus values. These values are computed by convolving at each wavelength, the spectral energy of a source with each of the three color matching functions, denoted as $(\bar{x}, \bar{y}, \bar{z})$, and illustrated in Figure 5. In this figure, you can see that the curve and peak of $\bar{y}$ is equal to Vλ. Tristimulus values are calculated using the following equations: [26]

$$\boldsymbol{X = K \sum_{\lambda=380}^{760} (S(\lambda)\bar{x}(\lambda))}$$
$$\boldsymbol{Y = K \sum_{\lambda=380}^{760} (S(\lambda)\bar{y}(\lambda))}$$
$$\boldsymbol{Z = K \sum_{\lambda=380}^{760} (S(\lambda)\bar{z}(\lambda))}$$

Equation 5: Tristimulus Values

where

$$K = \frac{100}{\sum_{\lambda=380}^{760} (S_w(\lambda)\bar{y}(\lambda))'}$$

$S(\lambda)$ Spectral energy of the object specified

$S_w(\lambda)$ Spectral energy of adapting white light source

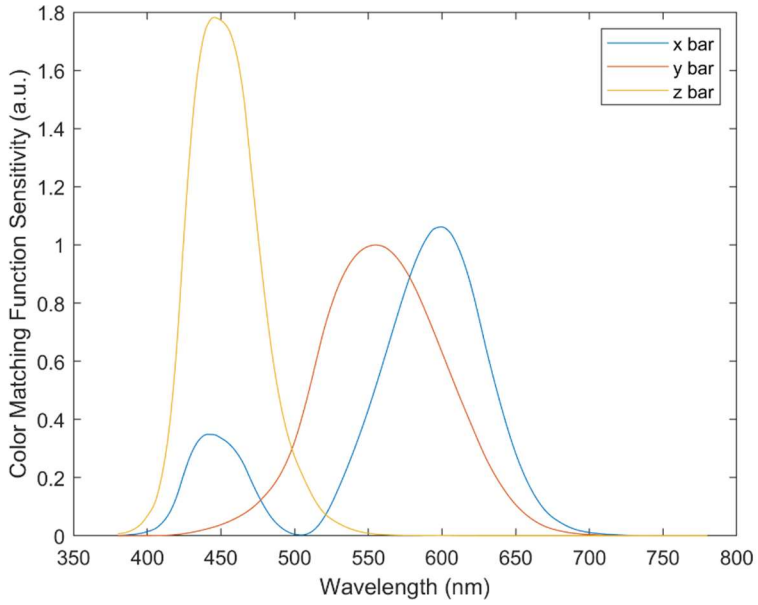

Figure 5: Color Matching Functions (MATLAB)

The tristimulus values aren't very intuitive by themselves. Since Y = Vλ, a large Y indicates a brighter color. In addition, the closer the values of X, Y, and Z are to each other, the more neutral the colors of the light. Beyond this, it is difficult to interpret the tristimulus values without a transformation. The transformation yielding more useful information produces chromaticity coordinates (x, y, z) within the 1931 CIE color space. This color space is especially useful in color science since each color can be represented numerically within the space. This transformation is performed as follows:

$$x = \frac{X}{X+Y+Z}$$
$$y = \frac{Y}{X+Y+Z}$$
$$z = \frac{Z}{X+Y+Z}$$

Equation 6: Chromaticity Coordinates

Since the CIE coordinates always sum to 1, x and y are sufficient for a complete description of color. Thus, we use a 2-dimensional CIE chromaticity diagram, as shown in Figure 6, to draw conclusions about the representation of color. Luminance is not represented in this color space and as a result, neither is the directly additive nature of the colors. Therefore, luminance must be represented to add colors in this space. In this research, two emitters, each with their own coordinates and luminance values, are used. These emitters are represented by a single set of x and y coordinates by adding the colors of the individual emitters. This assumes that we are modeling a lamp which includes 2 emitters, which each emit a portion of the light output by the lamp. The following equation shows how the composite x and y are computed:

Color Mixing Notation

$$x = \frac{\frac{m_1 x_1}{y_1} + \frac{m_2 x_2}{y_2}}{\frac{m_1}{y_1} + \frac{m_2}{y_2}}$$

$$y = \frac{\frac{m_1 y_1}{y_1} + \frac{m_2 y_2}{y_2}}{\frac{m_1}{y_1} + \frac{m_2}{y_2}}$$

Equation 7: Color Mixing Notation

where

x_1, y_1 $\quad$ $Chromaticity\ coordinates\ for\ color\ 1$

x_2, y_2 $\quad$ $Chromaticity\ coordinates\ for\ color\ 2$

m_1, m_2 $\quad$ $Luminance\ values\ of\ colors\ 1\ \&\ 2\ respectively\ where\ m_1 is\ 1$

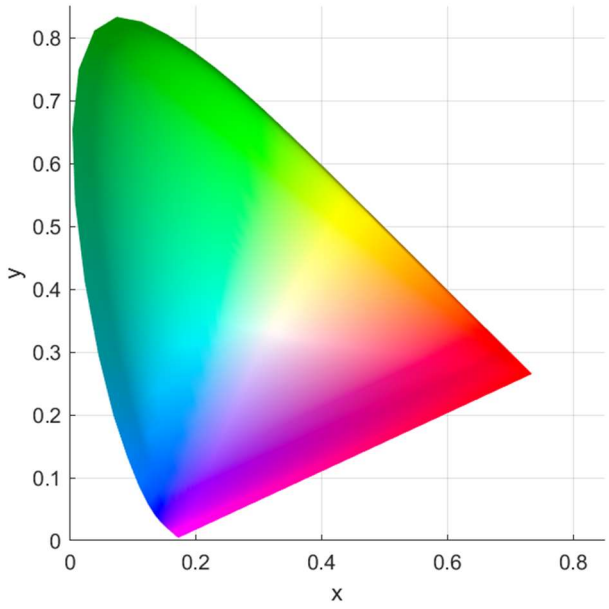

Figure 6: CIE Chromaticity Diagram (MATLAB)

To summarize the 1931 CIE Chromaticity color space, some assumptions can be made to simplify the interpretation of values. If the x and y results from Equation (7) are low, it indicates that the color is likely to be perceived as blue, whereas higher x, lower y values will appear red, moderate values of x and high values of y will appear green, and moderate values, specifically values around 0.33, of both x and y will appear neutral (gray or white) [26].

We can compute x and y based upon the peak wavelengths, bandwidths, and relative emission of the two emitters. Therefore, once we have characteristics for one emitter, we use Equation (7) to solve for the luminous intensity (m2) of the second emitter. Since we are interested in creating light which is perceived to be white rather than red, green, or blue, this approach limits solutions to colors near white. The American National Standards Institute (ANSI) defines a range within the color space to be considered D65, i.e., neutral gray or white. The standard requires a reference or correlation to the "equal energy white" color point at x = y = 0.33 known as D65. We define this space with a parallelogram referred to as the ANSI or D65 parallelogram or box in this work. This parallelogram defines the standards limits of color points considered D65. For our case using two emitters, the colors in or on the boundaries of the ANSI parallelogram are determined by computing the ratio of the emitters.

The amount of energy used to produce the light is related to the efficiency of the emitters. However, it is more beneficial for our purposes to determine how efficiently the emitter produces luminance levels that the human eye is sensitive to, otherwise known as efficacy. The computation of both efficiency (E) and efficacy (E_a) require optical power (P_o), electrical power (P_e), and luminance, and are formulated using Equation (8). Since we do not have a representation of the electrical power of our lights, we cannot use these equations as they are. Instead, we compute the luminance for our light source divided by the luminance of a 560nm emitter (L_{e560}) having the same optical power. The result of this may be best described as relative efficacy (E_r), and is calculated using Equation (8).

$$E = \frac{P_o}{P_e}$$

$$E_a = \frac{L}{P_e}$$

$$\boldsymbol{E_r = \frac{L}{L_{e560}}}$$

Equation 8: Efficiency & Efficacy

where,

E	Efficiency
E_a	Efficacy
E_r	Relative Efficacy
P_o	Optical Power
P_e	Electrical Power
L	Luminance

Now that the color space and its corresponding metrics have been defined, the process of defining the problem will help demonstrate how and why this space was chosen to investigate. The progression of this research began with determining where and what space was available to improve lighting in the built-environment to consider the non-visual effects. The literature referenced in the chapter II review sheds light on the specific circumstances in the ISR profession. The need to increase circadian rhythms without compromising detail detection was apparent. This led to electing the LRC's model for computing circadian effects of simulated emitters as the primary model. The range in the visible spectrum that the ipRGC's are sensitive to was obtained from Rea. This information helps represent the range of wavelengths that the ipRGC's are sensitive

to and result in non-visual effects by influencing the production or suppression of melatonin.

The methodology of this work creates various candidate lamps by varying the peak wavelength, bandwidth, and intensity of two Gaussian-shaped emitters. The normalized intensity of the resulting spectra for each lamp is used to calculate the optical power necessary to obtain a desired illuminance. This lamp output is then evaluated to determine if it produces light which is acceptable in color. Finally, the dependent measures for this candidate lamp are calculated. These steps including inputs and outputs are visually depicted in Table 3. Using the 1931 CIE color space permits us to precisely determine the location of the emission. The center of the wavelength or peak for an emitter, determines where the emitter point is on the diagram. Changing the bandwidths of these emitters moves the color produced by these emitters around the color space. As these parameters for each of the two emitters change, the color of light emitted changes. In addition, the relative peak heights of the two emitters necessary to achieve white light emission changes. To compensate for this CCT change, we adjust the relative amplitude of the yellow emitter peak.

To visually analyze the multiple dimensions of the problem a model was constructed to manipulate the independent variables to determine their effects on the dependent variable. This was done to better understand the overall influence of the independent variables on the dependent variables. This analysis allowed us to draw insight and discuss the trends in the data in this early analysis but placed no constraint on the color of the light produced. As a preliminary action we then used the LRC's model to compute CLA as a function of the spectrum of light at the human's eye, the illuminance

level in lx at the human eye, and melanopsin sensitivity data. The results indicate that changing the bandwidth of the blue moves it away from the chromaticity space boundary and towards D65 white, but not in a straight line as seen by three chromaticity plots in Figure 7. The circadian light intensity value is also determined in this function.

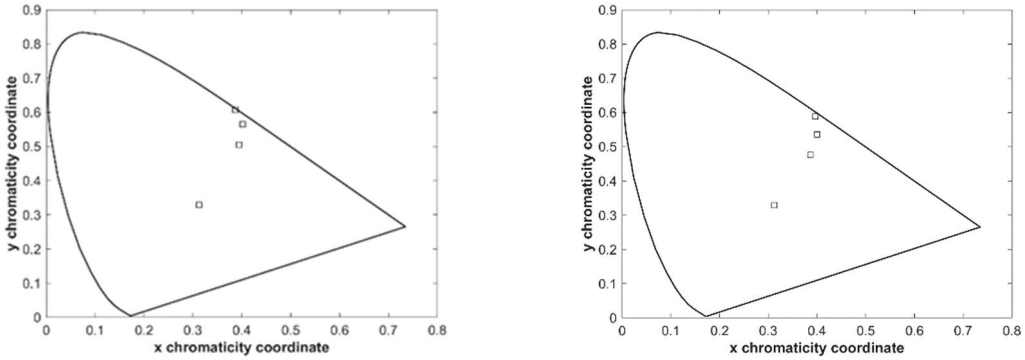

Figure 7: Demonstration of how changing yellow bandwidths moves emitters with two separate wavelengths non-linearly away from or toward D65 (shown as the point nearest the center).

The model was modified to manipulate the independent variables while constraining the color. This provided data that contained values representing color, relative efficacy, and CS. We were then able to apply regression analysis to the data as a way of determining optimal values.

In this step, the model was extended to ensure the color of light was within the ANSI specified region of D65 white light. We now evaluate the space between the two emitters by drawing a straight line between them. Along this line the ratio of the luminance produced by these two emitters can be used to determine the color point to achieve white light. The line between the color coordinates of the two emitters must intersect with D65 to provide illumination which meets the ANSI standard for D65 illumination. The coordinates of the emitters were moved systematically through the x

and y space. If an intersection with the D65 box occurred, the model returns two sets of coordinates: one for each side of the D65 box that the line intersects. Intersecting and non-intersecting scenarios are shown in Figure 8.

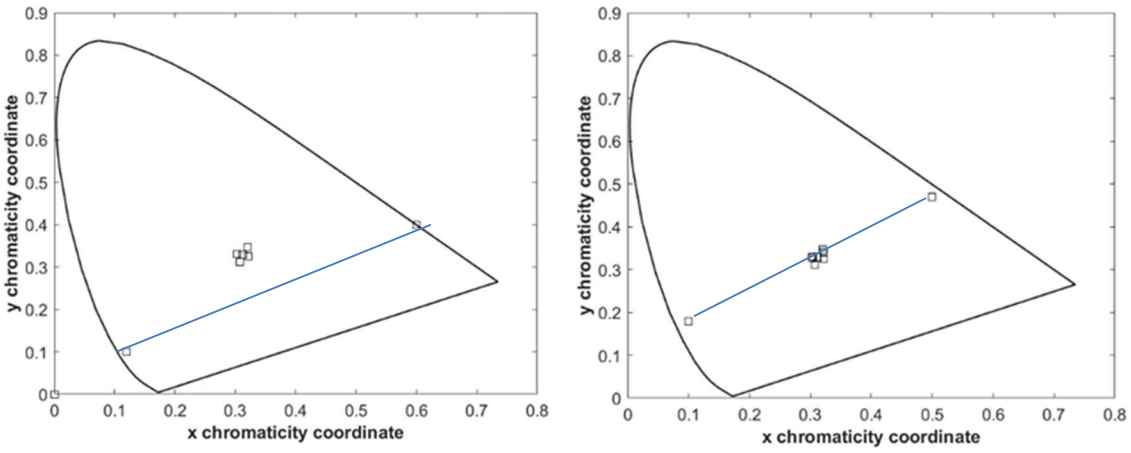

Figure 8: ANSI Intersect Box Test showing an intersecting (right) and non-intersecting (left) pair

After identifying all pairs of wavelengths from the two emitters that intersect with the D65 box, the results were organized into a matrix. In this matrix, shown in the leftmost portion of Table 5, columns 1 and 2 contain the chromaticity coordinates of intersection of the line with the D65 box. Columns 3 and 4 contain the index values for the chromaticity coordinates of the emitters. These coordinates are used to look up values in the right two lists in Table 5.

Table 5 contains three matrices that contain the values needed for the color mixing calculations. The odd rows in the matrix labeled emitter points (EPts) contain the x and y coordinate values of where that blue emitter intersects the D65 region and the even rows are the same for the yellow emitter. Columns 3 and 4 contain the index values for the other two matrices. A value of 1 and 2 in the third and fourth columns of EPts

directs us to the first and second row of bxyzc for the blue emitter and yxyzc for the yellow emitter. The values contained in bxyzc and yxyzc are the coordinates of the emitters themselves.

Table 5: Intersect Output Data Test

EPts			
0.3214	0.3254	2	1
0.3221	0.3266	2	1
0.3197	0.3238	3	1
0.3220	0.3279	3	1
0.3177	0.3219	4	1
0.3219	0.3293	4	1
0.3153	0.3195	5	1
0.3217	0.3310	5	1
0.3123	0.3167	6	1
0.3216	0.3330	6	1
0.3088	0.3133	7	1
0.3214	0.3353	7	1

bxyzc		
0.1552	0.0195	0.8254
0.1544	0.0207	0.8249
0.1535	0.0223	0.8242
0.1525	0.0243	0.8232
0.1513	0.0269	0.8218
0.1501	0.0301	0.8198
0.1488	0.0339	0.8173
0.1475	0.0384	0.8140
0.1463	0.0437	0.8100
0.1450	0.0498	0.8052
0.1440	0.0566	0.7994
0.1430	0.0641	0.7928
0.1424	0.0723	0.7854
0.1420	0.0809	0.7771
0.1420	0.0900	0.7680
0.1423	0.0994	0.7583
0.1430	0.1090	0.7480
0.3127	0.3290	0.3582

yxyzc		
0.4459	0.5526	0.0015
0.4467	0.5516	0.0017
0.4474	0.5506	0.0020
0.4481	0.5495	0.0024
0.4486	0.5485	0.0029
0.4490	0.5474	0.0036
0.4492	0.5464	0.0045
0.4492	0.5452	0.0056
0.4489	0.5439	0.0072
0.4485	0.5424	0.0091
0.4477	0.5406	0.0116
0.4468	0.5385	0.0147
0.4455	0.5360	0.0185
0.4439	0.5330	0.0231
0.4420	0.5297	0.0283
0.4399	0.5258	0.0343
0.4375	0.5216	0.0410
0.3127	0.3290	0.3582

The values in the outputs of Table 5 were used in Equation (7) color mixing notation to solve for m_2 representing the luminous intensity of the second emitters assuming the first emitter is 1 lx. This result was placed in the fifth column of the emitter points output to position the most useful values in one place for a stepwise evaluation procedure. The area constant of the two-emitter mixture as a function of wavelength range, the center wavelengths and widths of blue and yellow, and the m_2 luminous intensity was placed in column 6. Relative efficacy was computed via the integration of the Vλ function by the emitters wavelengths across all wavelengths and placed in column 7. The CRI of the emitter spectrum with respect to a reference light with standard 8

patches as well as 15 patches reside in column 8. The CLA and CS values are placed in the final two columns, 9 & 10.

The multiple regression was conducted in two phases. Phase I was accomplished by creating a program in MATLAB which synthesizes theoretical spectra at desired illumination levels and computes several important criteria for each spectrum, including CLA, CS, the color of light, efficacy of light, and color quality using the CRI. This model permits CS values to be calculated which can be obtained by increasing luminance or changing the wavelength of the light. Phase II applied multiple regression techniques in JMP to explore the solution space for the output of the MATLAB model.

The MATLAB model generated visible light spectra between 360 and 780 nm in 1 nm increments. These spectra were comprised of two Gaussian-shaped peaks, representing a short and a long wavelength emitter. The model permitted the center wavelength of the short wavelength emitter to be varied between 380 and 480 nm and a long wavelength emitter having a center wavelength which is varied between 540 and 640 nm in increments of 5 nm. The full width at half maximum amplitude bandwidth of each emitter was also varied between 20 and 100 nm in increments of 5 nm. The resulting two emitters produced light with color illustrated by the two ellipses in the CIE chromaticity diagram shown in Figure 9. As shown in this figure, the short wavelength emitter produced light with colors that are generally within the cyan ellipse while the long wavelength emitter produced light with colors that are generally within the yellow ellipse.

The D65 parallelogram is roughly represented by the square region near the center of the CIE diagram shown in Figure 9. If the line did not intersect this region, the pair

was discarded. If the line intersected this region, the intersection points were calculated. The relative intensity of the two peaks needed to achieve the color of light at the intersection points were then calculated using Hunt's Center of Gravity Law [8]. Finally, the intensity of the spectra was adjusted to produce the desired intensity of 250 lx. The resulting spectra that produced light having a color on the edges of the D65 parallelogram were then analyzed further.

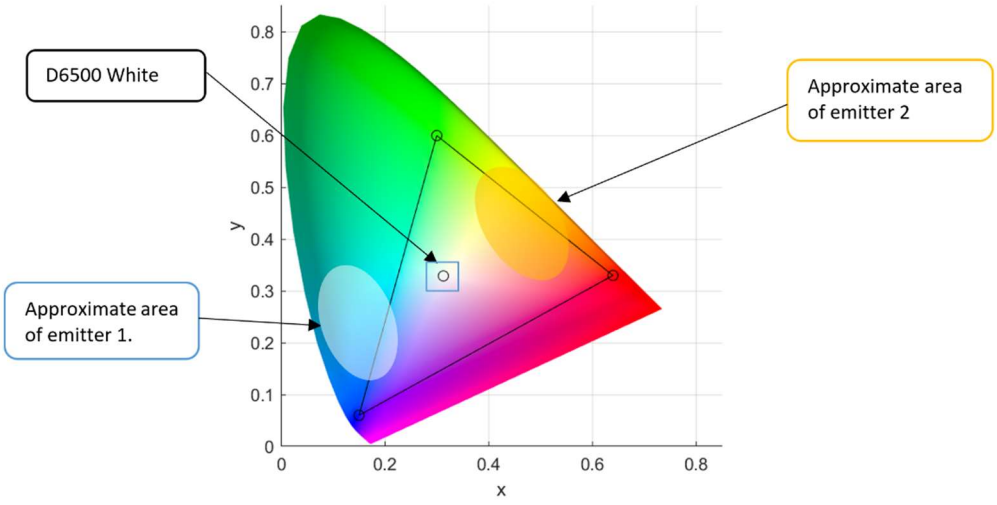

Figure 9: Emitter & D65 Locations in Color Space

For each selected spectrum, CLA, CS, relative efficacy, and CRI were calculated. The CLA, CS, and CRI were calculated as discussed in previously cited articles. It is worth noting that CS varies between 0 and 1 with 0 representing no stimulation of the human circadian system and 0.7 representing full stimulation (saturation) of the human circadian system. To maximize alertness, a value of 0.7 is therefore, desired. CRI varies between some negative value and 100. Generally, minimally acceptable values for illumination are about 70. Relative efficacy is intended to represent the efficiency of a

lamp having the desired spectrum. As these emitters are theoretical, we did not attempt to estimate the electrical power necessary to produce the desired illumination. Instead, we computed a metric, we refer to as relative efficacy, which represents the efficacy of the illumination as it is viewed by the human eye. This metric involved convolving the spectrum with the photopic sensitivity function for the human eye, integrating the result across the visible spectrum, and dividing it by the integral for the photopic sensitivity function of the human eye. The resulting metric varied between 0 and 1 where 1 would be created by an infinitesimally narrow emitter having a peak at the peak sensitivity of the human eye.

In summary, the variables of measurement for the regression analysis include the five independent variables of center wavelength and bandwidth for each emitter (for two emitters, these are four separate values), and the ratio of luminous intensity between emitters. Dependent variables of interest include the circadian stimulus, CRI, and relative efficacy. However, solutions of interest will have a high CS but with desirable levels of CRI, relative efficacy, and color of illumination.

In Phase II, multiple regression analysis was applied to examine the potential spectra generated during Phase I. Multiple regression analysis is a predictive analytics technique that allows us to estimate a function that describes the relationship between our dependent variable (CS) and multiple independent variables (e.g., blue and yellow emitter peaks, blue and yellow widths, and ratio of luminous intensity). The regression was performed and adjusted with additional parameters as analyses shed light on outliers, trends, and interactions among the dependent measures.

Referring to the D65 parallelogram discussed earlier, there are five sets of coordinates identifying the parallelogram with the four corners and the center point. We further developed a programmed loop to return all feasible pairs of blue and yellow wavelengths that intersect with the D65 parallelogram, followed by the most desirable of these emitter pairs, their tristimulus values, chromaticity coordinates, and efficacy. This will be the feasible region of interest to which optimization methods are applied. The luminous efficacy is then obtained by the integration of the Vλ function by emitters across all wavelengths in the visible spectrum. The output of this paired wavelength selection function provides the coordinates of the emitters and of the points of intersection with D65 on both sides of the parallelogram. This information is used to compute the luminous intensity of the second emitter where it is assumed that the first emitter is equal to 1. Finally, the CRI is calculated for each desired emitter. The range of emitters this is computed for is crafted to assess the tradeoffs between CS, CRI, and efficacy. Although the aim of this work is to determine an optimal CS and CRI, this optimization can be engineered using these inputs for different scenarios allowing different brightness levels.

In the Phase III we then modified the model to apply a genetic algorithm on our dependent and independent variables to create a pareto front. This multi-objective approach filters the potential emitter pairs for non-dominated combinations of CS, CRI, and efficiency. The parameters of the problem are represented in global variables where we constrained the inputs to particular ranges of wavelengths within the visible spectrum. Initial input values cause the algorithm to begin in the ANSI parallelogram. Once the space is well defined with this output and the pareto front is identified the input values

will be adjusted to further illustrate the trade-offs associated for losses and gains in each variable. We then input a fourth variable to the model to consider color based on the distance between D65 and the color of the emitter as another measurement of color. This was done using a Euclidean distance equation to measure the distance between the line segment of D65 and the emitter, and then attempting to minimize this value to increase the quality of the color.

It is important to note that there are some differences in how wavelengths were defined in the programming portion of work between regression and optimization analyses. In the genetic algorithm pareto front we permitted the blue emitter center wavelength to vary from 380 to 500, the yellow emitter center wavelength to vary from 500 to 760, and the bandwidths to vary between 5 and 200 nm. The yellow luminance ratio was also allowed to vary between .0001 and 100. The code used to form desired emitters for multiple regression output were limited so that blue and yellow emitters widths could not exceed 100 nm, blue center wavelengths varied between 380 and 480, and yellow varied between 540 and 640.

Summary

The model-driven procedure for generating optimized emitter pairs, and the methodology for collection and analysis of its supporting data utilize a mixture of methods. These include regression and multi-objective nonlinear optimization to produce and analyze a pareto front. The non-visual effects of short wavelengths of light are analyzed to optimize the CS output of a light source with a constant target illuminance. If an effective increase in CS can be achieved with a constant input

illuminance, this knowledge can be leveraged to educate decision makers, managers and individuals. This sharing of knowledge can modify exposure to short wavelengths of light in work centers and homes to promote enhanced circadian rhythms.

IV. Analysis and Results

Chapter Overview

This chapter summarizes and discusses the results of the optimization of CS in three phases. The first phase focused on the parameters of the space, the second on regression analysis to understand variable relationships, and the third on optimization. Results are provided for CS, CRI, relative efficacy, and at times color difference for desired emitter pairs at illuminance levels of both 250 and 21.5 lx. Two sets of data are compared where the standard illuminance of two different settings is used to highlight that illuminance and CS are best represented by a logarithmic relationship. Finally, recommendations are made to existing standards to leverage LED technology to enhance circadian rhythms.

Figure 10 illustrates a reference for later comparison using the spectral data of a white LED spectrum close to D65. The data represents what you might typically find in the spectral output of a D65 LED placed overhead in a workspace, This particular light produces a CS of 0.277, CRI of 63.5, and relative efficacy of 0.656 at 250 lx. We will see how our model is selecting emitters that provide a better CS, CRI, relative illuminance, and is closer to the ANSI D65 region than this reference D65 in Figure 10.

Models were manipulated during Phase I to observe and visualize the space to be explored during the optimization. The LRC's model was used to calculate CLA and CS. The output was used as a validation set to ensure CLA and CS values were accurately matched to the LRC's CS calculator [29]. The output for CLA and CS values are produced in 8x3 matrices with columns representing the intensity of the yellow emitter

peak and rows representing the bandwidth of the blue emitter. The resulting CLA and CS values are plotted in Figure 11 to analyze the behavior of the two variables. Note that this supports the understanding that CLA and CS have a logarithmic relationship that asymptotes as CS approaches 1. This makes sense when referring back to the calculation of CS in Equation (3) from Chapter 2.

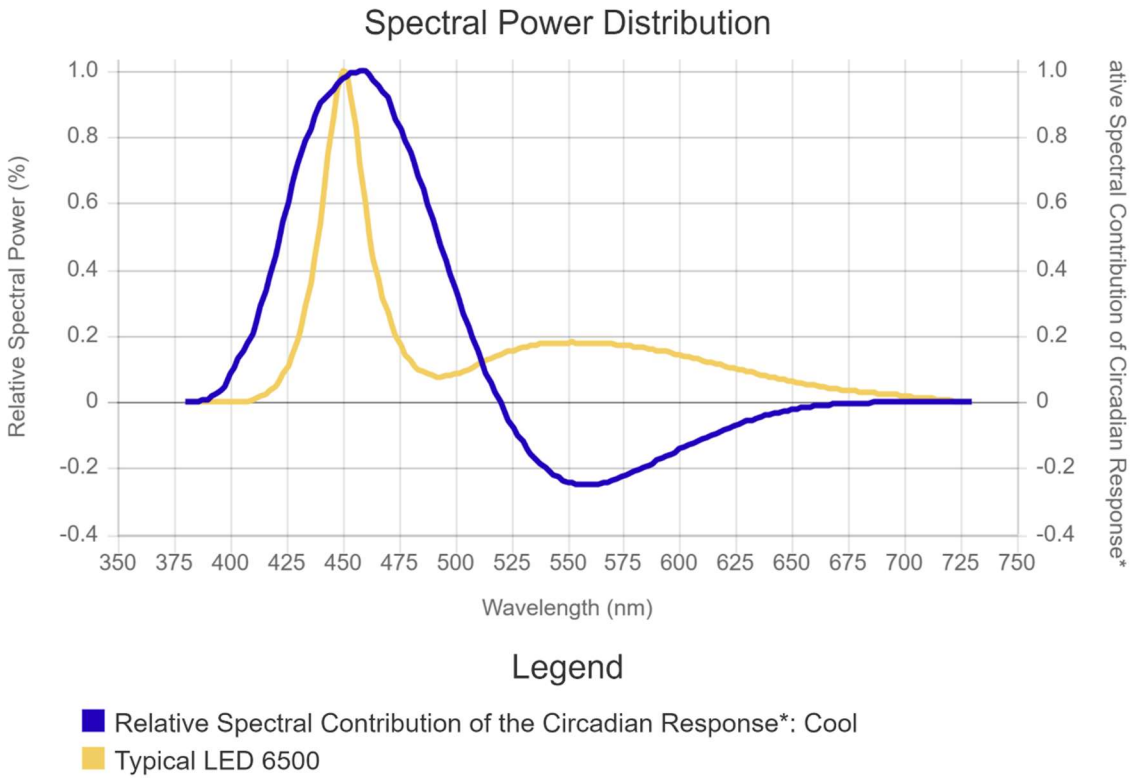

Figure 10: Relative spectral power for a white LED and relative spectral contribution of circadian response as a function of wavelength from the RPI LRC calculator [30].

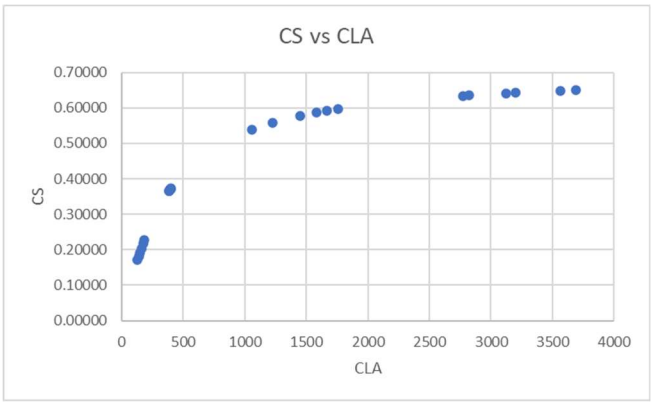

Figure 11: Circadian stimulus (CS) as a function of circadian light (CLA)

The model in Figure 12 graphically represents CS as a function of yellow emitter peak intensity and bandwidth of the blue emitter with a constant illuminance of 21 lx. This model confirms that increases in yellow peak height relative to fixed blue peak height of 1 reduces CS for a given illuminance value. Lower yellow emitter peaks and increases in blue emitter bandwidth increase CS as these manipulations increase the shorter wavelength blue energy to which the ipRGCs are sensitive. Desirable CS values (CS > 0.3) can be achieved at 21.5 lx, although the light that is produced presents as much more blue than white as CS increases. This tradeoff explains that targeting increased CS levels with low levels of illuminance will yield illumination that is bluer in color than yellow. Within this process we are holding illuminance constant at a single value, but allowing the relative peak heights and widths of blue and yellow to vary within a range. The takeaway from Figure 12 is if color is not constrained, CS values near 0.3 can be attained at an illuminance of 21.5 lx.

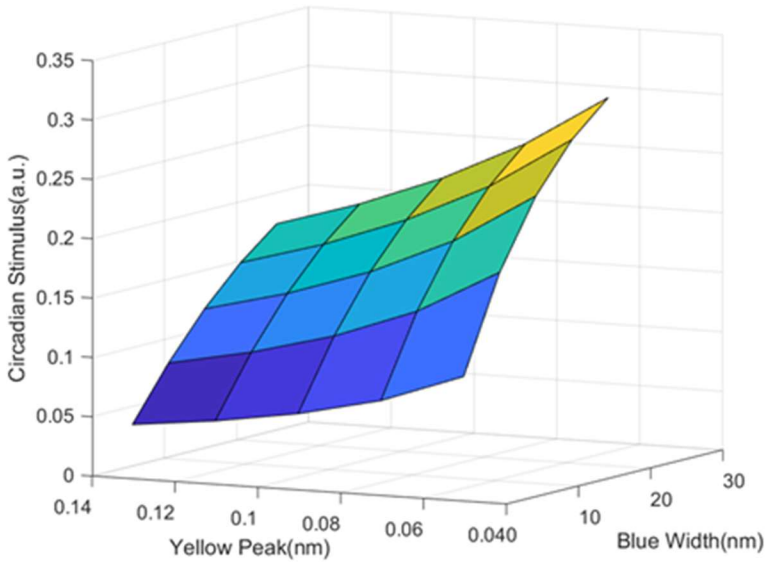

Figure 12: CS as a function of the yellow peak height and bandwidth of the emitter at an illuminance of 21.5 lx. Yellow peaks are in units relative to the blue peak height of 1.

Output with Color Constrained to D65 box edges

When programmed to include all blue emitter center wavelengths between 380 nm and 480 nm and yellow emitter center wavelengths between 540 nm and 640 nm in steps of 5 nm, the model generated 6776 possible pairs. When placed in descending order from highest to lowest CS, the four top entries are shown in Tables 6a, 7b, and 8c. This was repeated for three separate illuminance values of 21.5 lx, 250 lx, and 500 lx in Tables 6a, 7b, and 8c, respectively. The top values of CS when color is constrained to D65 at 21.5 lx is CS = 0.07, a CS = 0.43 for 250 lx, and CS = 0.55 for 500 lx. These values compare to the plot in Figure 11 where the color of light is not constrained. As shown, it is not feasible to achieve the target CS value of at least 0.3 at 21.5 lx while producing light that is considered D65 in color. Therefore, higher levels of illuminance, specifically

illuminance levels near 250 lx will be required to obtain a CS of 0.3 if D65 illuminance is required.

Table 6a: Feasible Emitter Pair's Maximum CS at Input Illuminance of 21.5 lx

x	y	b index	y index	m2	calcC	Efficacy	CRI	CLA	CS
0.306588	0.312311	341	187	3.855575	0.181315	0.142461	31.2654	47.80361	0.069018
0.30648	0.312827	341	165	3.799862	0.208645	0.140826	27.74793	47.36184	0.068384
0.306556	0.312467	341	137	3.758718	0.644173	0.139619	-2.79924	47.18166	0.068125
0.306419	0.313119	341	138	3.775525	0.521103	0.140112	0.505432	46.96192	0.067809
Illuminance = 21.5 lx									

Table 7b: Feasible Emitter Pair's Maximum CS at Input Illuminance of 250 lx

x	y	b index	y index	m2	calcC	Efficacy	CRI	CLA	CS
0.306588	0.312311	341	187	3.855575	0.181315	0.142461	31.2654	569.2115	0.438742
0.30648	0.312827	341	165	3.799862	0.208645	0.140826	27.74793	563.3959	0.436885
0.306556	0.312467	341	137	3.758718	0.644173	0.139619	-2.79924	559.7403	0.435706
0.306419	0.313119	341	138	3.775525	0.521103	0.140112	0.505432	557.2288	0.434889
Illuminance = 250lx									

Table 8c: Feasible Emitter Pair's Maximum CS at Input Illuminance of 500 lx

x	y	b index	y index	m2	calcC	Efficacy	CRI	CLA	CS
0.306588	0.312311	341	187	3.855575	0.181315	0.142461	31.2654	1166.248	0.551176
0.30648	0.312827	341	165	3.799862	0.208645	0.140826	27.74793	1153.236	0.549722
0.306556	0.312467	341	137	3.758718	0.644173	0.139619	-2.79924	1142.741	0.548528
0.306579	0.312354	342	187	3.756802	0.229102	0.180982	36.51636	1138.24	0.548011
Illuminance = 500lx									

Phase II applied multiple regression analyses to better understand the effect of emitter parameters on CS. Assumptions of regression were adhered to: i.e., linear relationship is suspected, outlying data is assessed and properly handled, independent variables possess little to no collinearity, residuals present homoscedasticity, and the residual distribution appears normal. The initial regression model included all wavelength pairs that intersect with the D65 region. This initial regression was performed with CS as the dependent variable and luminous intensity, the center wavelengths and bandwidths of

each emitter as the independent variables. The resulting model is shown in Figure 13a. As shown, there are several outliers which were separate from the main body of observations on the plot. As these outliers, are not near the maximum CS values, a second model constrained the inputs to values which had a CRI greater than 40 and relative efficacy greater than 0.4. The resulting model is depicted in the left panel of Figure 13. As shown the maximum CS value is about 0.42. Eliminating the emitters with low CRI values eliminates emitters across all CS Values but values near the maximum CS value of 0.42 remain.

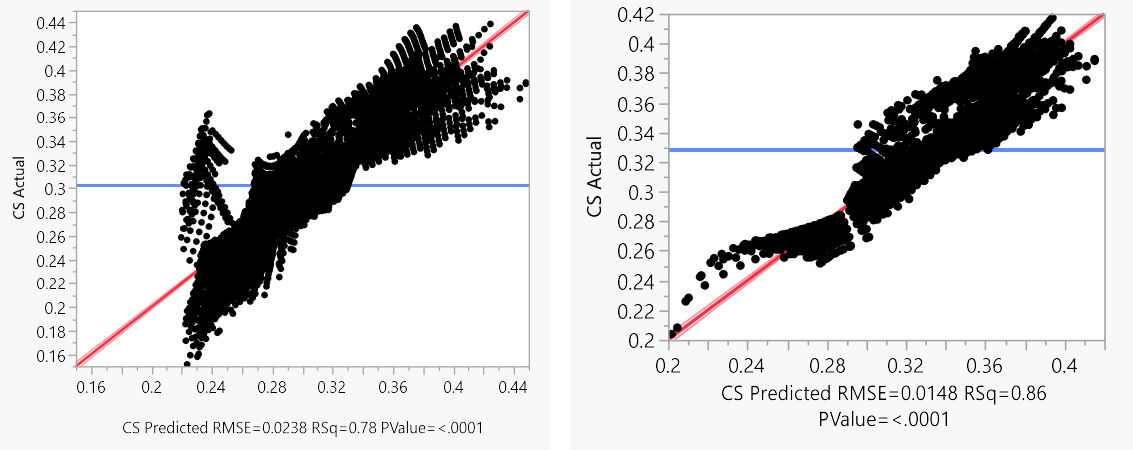

Figure 13: Results of multiple regression including all spectra on the (left) and all spectra with a CRI >40 (right). Each point represents a selected emitter pair.

A final model is shown in the right panel of Figure 13. In this model, the emitters are constrained to CRI > 70 and relative efficacy > 0.4. Although a single model is fit, the figure shows two separate clusters of emitters. The top cluster has CS values between about 0.35 and 0.40. The lower cluster has CS values between about 0.29 to about 0.36. The cluster having higher CS values generally include blue or short wavelength emitters having center wavelengths between 460 and 480 nm with bandwidths between 50 and

100 nm. The yellow or long wavelength emitters for the spectra within this cluster have center wavelengths of 575 to 610 nm with bandwidths ranging from 55 to 100 nm. The ratio of the luminance of the long wavelength emitter to the luminance of the short wavelength emitter for spectra within the top cluster had an average of 2 and a maximum value of 9.3.

The lower cluster included similar emitters, except the center wavelengths of the blue or short wavelength emitter ranged from about 425 to 480 nm and the ratio of the luminance of the long wavelength emitter to the short wavelength emitter had an average of 5.3 with a maximum value of 20, which is high in comparison to the upper cluster. Relative efficacy and CRI remained relatively similar between the clusters, but CS values were consistently higher for emitters which included more energy in the lowest wavelength emitter. This is consistent with the initial analysis.

The top cluster from Figure 14. is shown in Figure 15. As shown, this cluster of points are generally clustered around the line determined from the linear regression which results in the equation:

$$\mathbf{Y = 0.4779 - 0.0021\ BCW - 0.0012\ BBW + 0.0018\ YCW - 0.0004\ YBW - 0.0074LR}$$

Equation 9: Regression Prediction Equation

where BCW is the blue center wavelength, BBW is the blue bandwidth, YCW is the yellow center wavelength, YBW is the yellow bandwidth and LR is the ratio of the luminance of the yellow emitter to the luminance of the blue emitter. As this equation illustrates within the range of the values in this cluster, shorter blue center wavelengths,

longer yellow center wavelengths, and smaller bandwidths, together with lower luminance ratios result in higher CS values.

The point in Figure 15 with the maximum CS value has a value of 0.40, a CRI of 70.7, a relative efficacy of 0.47. It is comprised of a short wavelength emitter having a center wavelength of 480 nm with a bandwidth of 65 nm and a long wavelength emitter having a center wavelength of 595 nm and a bandwidth of 90 nm. The luminance output of the long wavelength emitter is 2.1 times the luminance output of the short wavelength emitter, which allows it to achieve D65 as its color. Interestingly, a typical commercially available white LED having a similar color temperature tends to have a short wavelength emitter with a center wavelength near 440 to 450 nm with a bandwidth around 20 nm and a yellow emitter having a center wavelength around 590 nm with a bandwidth around 75 nm. Thus, the optimal emitter would have a blue emitter which is slightly longer in wavelength with a much broader emission than today's white LEDs.

It is worth noting that early versions of this model did not constrain the color of illumination. The optimal illumination inevitably resulted in blue rather than white light but permitted saturation of the CS value at similar illumination levels. This result is consistent with the finding that the ratio of the luminance of the long wavelength emitter to the luminance of the short wavelength emitter should be small. However, constraining the color to the color of light specified by Geospatial Intelligence lighting standards limits the range of CS values that can be obtained to values no more than 0.42 with an illuminance of 250 lx.

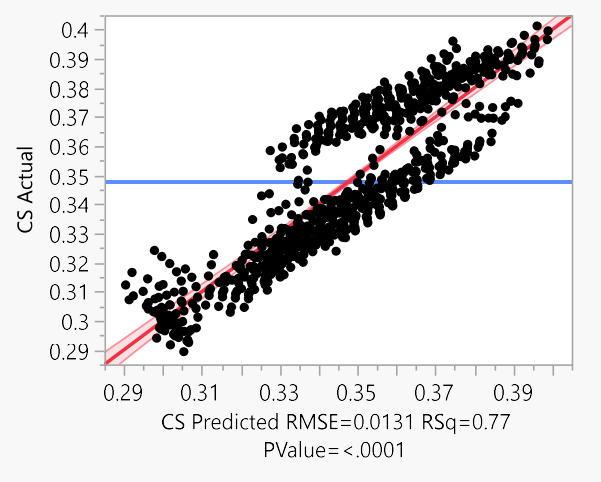

Figure 14: CS value as a function of predicted CS value for emitters having CRI > 70 and relative efficacy > 0.4. Note each point represents a selected emitter pair.

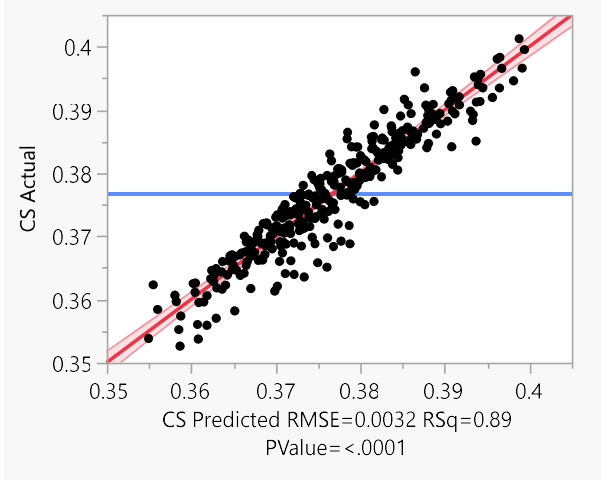

Figure 15: CS value as a function of predicted CS value for emitters in the top cluster shown in Figure 14. Note each point represents a selected emitter pair.

Now that this concludes the regression analyses, we will discuss the elements of each phase in the aggregate to highlight the importance and differences that led to each phase. Phase I: The emitter selection process was performed to obtain potentially viable emitter pairs, one placed in the blue region and one in the yellow. The blue emitter provides short wavelength energy that has primary influence on increased CS values while the yellow aids in balancing the brightness. Phase II: Regression analysis, using the emitter pairs from Phase I, enables assessment of the emitter pairs in a two-dimensional space. As seen in Figure 8, the line drawn between emitters in a viable emitter pair intersects the D65 box. This line intersects each side of the box and we gain solutions for these intersection points that are evaluated with regression. The limitation with this is that the color in the regression input is limited to just these D65 box edge solutions which does not allow us to assess any possible trades between color and CS.

Based on the relationships identified in the regression analyses, Phase III uses multi-objective analysis. The multi-objective optimization allows us to assess the tradeoff between color and CS. The MATLAB program that selects optimal wavelength pairs that intersect with ANSI D65 was extended to utilize a multi-objective genetic algorithm procedure that yields a pareto front. The pareto front generated in this way enumerates non-dominated emitter pairs that illustrate the optimal tradeoff between color and CS. The initial run considers CS, CRI and a new variable which measures color based on the distance in chromaticity of the resulting illumination emitter from D65. The distance between these points is measured with a Euclidean distance calculation. The smaller this distance value, the closer the color to D65. It is worth noting that the edges of the ANSI color box are between 0.01 and 0.02 chromaticity values from D65.

Figure 16 illustrates the pareto front of non-dominated emitter pairs. It plots CS, CRI, and color distance of these emitter pairs in multiple dimensions. This view is most useful for interpreting the relationship between CS and color distance, as it relates to CS: Some observations include: (1) As the distance of an emitter pair from D65 increases, so does CS. This is natural, since moving farther from D65 allows more of the CS rendering blue energy to be used. (2) Portions of the pareto front are planar. This can be seen more clearly in Figure 17. In this view, focusing on non-dominated emitter pairs in the CRI-CS plane, we see that as CRI decreases, CS increases. That is, among non-dominated emitter pairs, as the color of the light becomes less similar with respect to the reference D65 daylight, CS often increases. This is natural, driven by the same logic above describing how CS increases with the color distance from true white D65: In a non-dominated

emitter pair, the less similar the color is to D65, the more blue energy is available, which increases the CS.

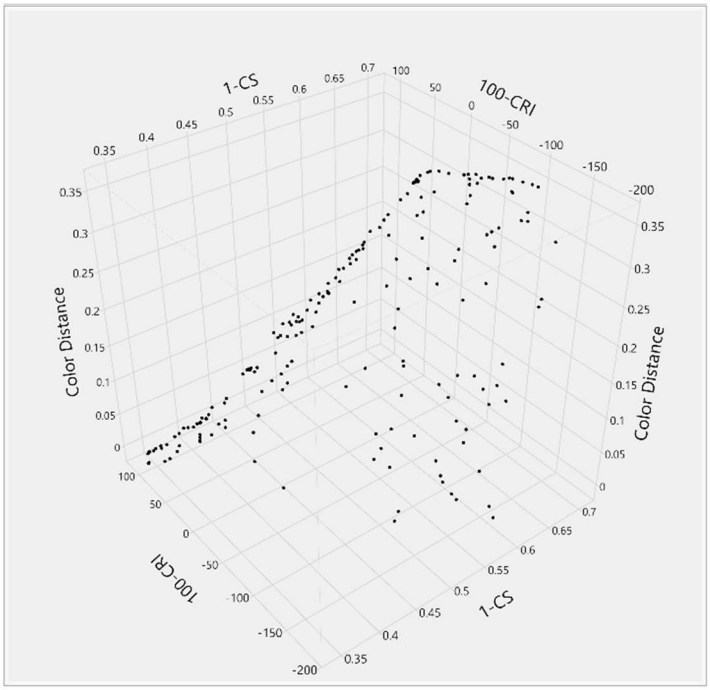

Figure 16: Pareto front for color distance, CS and CRI. Each point represents a selected emitter pair.

The relationship between CS with CRI and color distance is now explored to see how similar CRI and color distance are in determining CS. Since they indicate the same things, it is practical to interpret these relationships individually, and by their specific values which are shown in Table 9. The table includes the data sorted in order of descending CS from largest to smallest to further validate the fact that as CS increases, CRI decreases, and color distance increases.

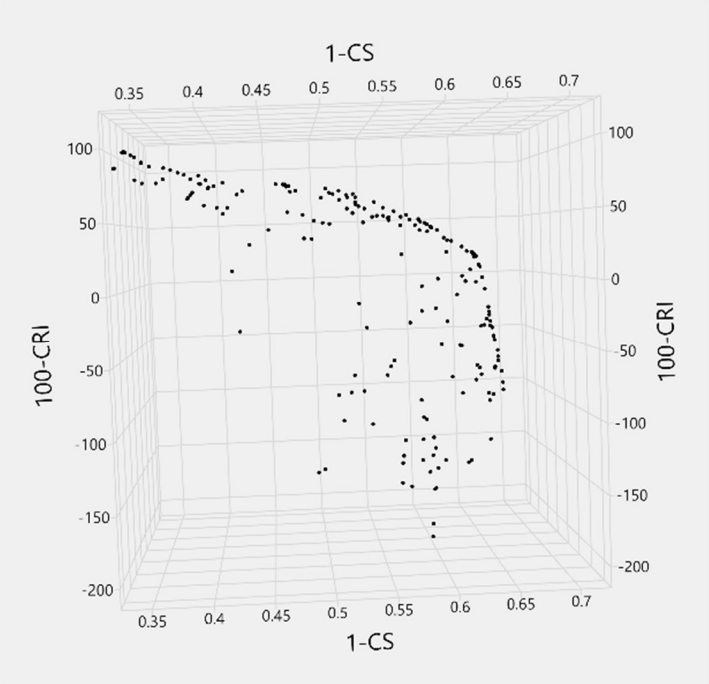

Figure 17: A rotation of Figure 16 to show a second view of the Pareto front.

Figure 18 shows some of the variability inherent in with the relationship between CRI and CS. In this restricted view of non-dominated emitter pairs, there is a generally downward sloping relationship. The variance among these increases substantially once CS reaches values greater than about 0.425. This supports the conclusion that CRI is quite important to include in the model. As we can see in Table 9, we can achieve favorable CS but with unfavorable color differences and CRI. This is illustrated by row 1 where CS is 0.7, color distance is 0.35 and CRI is -108. This point would appear in the lower right side of Figure 18. This plot is useful since our pareto front show us a favorable front where we can achieve CS values of up to approximately 0.475 before CRI begins to drop below 70.

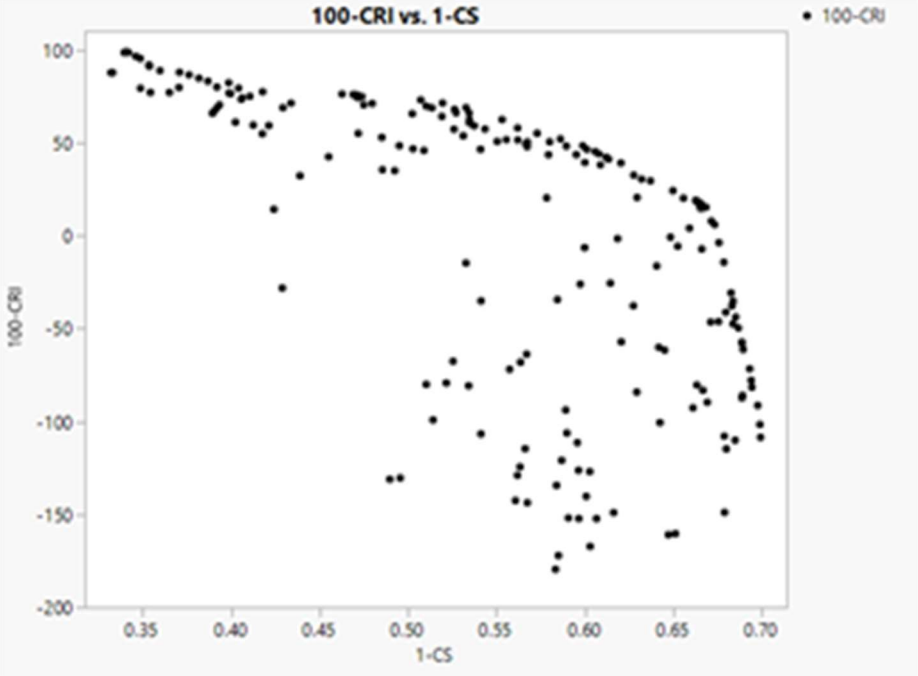

Figure 18: 1-CS against 100-CRI. Each point represents a selected emitter pair.

The plot from the multi-objective method in Figure 18 isolates the relationship color distance has with CS. The first observation is a tighter fit than Figure 18, which shows the relationship of CS and CRI along with an area of interest where distance is close to 0.00 and CS values are around 0.43 to 0.58. Next important observation is that this same increase in variance begins when reaching CS values greater than 0.425 which was seen in Figure 18 as well. After isolating the peak and width properties of the wavelengths associated with this area of higher variability, it was concluded that further research can be conducted to investigate this interaction, since no immediate characteristics of any variables could be identified at this depth of investigation. This

variability appears to be associated with the reaction the emitters color have once they reach a distance that places them outside the ANSI region of D65, therefore, we were unable to further constrain the data to improve the fit although these values possess a color distance that is not within the D65 region. For reference, the allowable color distance to remain within the D65 box is about 0.01 from the center for two corners and 0.02 for the other two corners. We see our pareto front does illustrate that we can obtain favorable CS values of up to approximately 0.375 before distances begin to exit the boundaries of the D65 region.

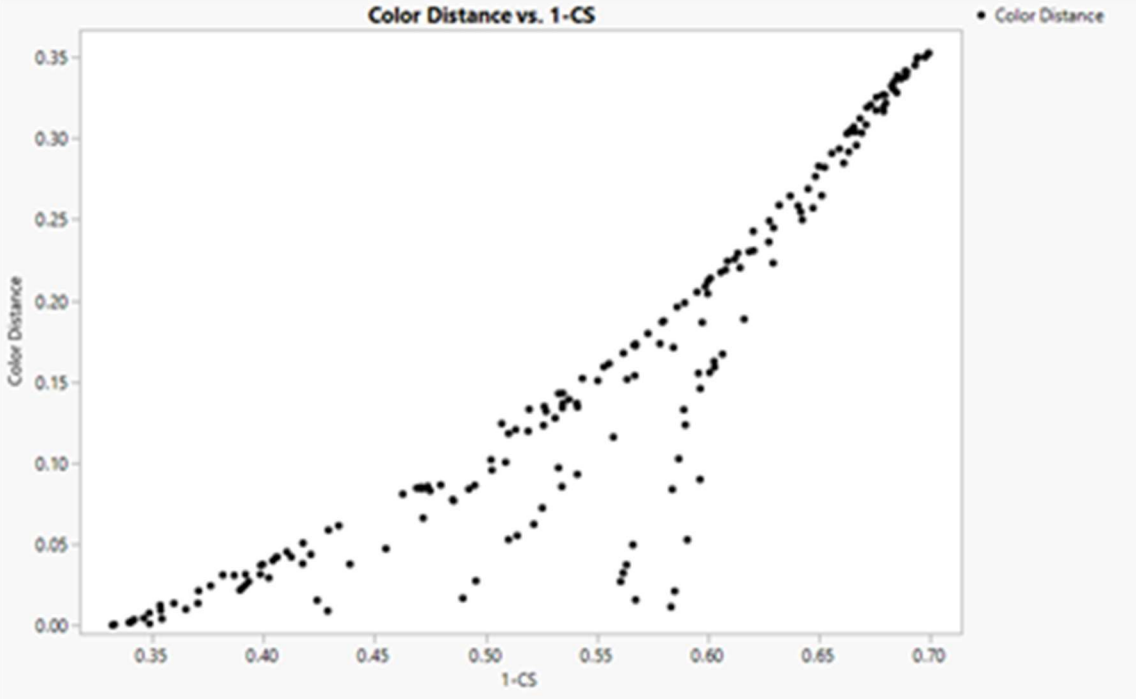

Figure 19: CS Against Color distance from D65. Each point represents a selected emitter pair.

Table 9: Variables Considered Individually

CS	CRI	Color Distance
0.699264	-108.5409641	0.352433865
0.698901	-101.6746359	0.351797592
0.697671	-91.41530504	0.349870306
0.694345	-81.60106135	0.349764373

Since color distance provides a closer linear fit with CS than CRI, we re-ran the genetic algorithm to consider only color distance and CS. The plot in Figure 20 illustrates that when the distance is around 0, the CS sits around 0.35. Studies done by the LRC consider high levels of light to be classified as $CS \geq 0.3$ and low light levels as $CS \leq 0.15$. This same study also deduces that lighting producing "$CS \geq 0.3$ can reduce sleepiness and increase vitality and alertness in office workers" [20]. With this is mind, we've already achieved values greater than 0.3 within the D65 region. At this point, we must see what tradeoffs are available to increase CS values so that they may be translated into lower levels of illuminance. We know the moment the distance increases, so does CS. This aligns with what we know so far. The drastic difference in CS which are obtained by increasing the distance by 0.15 would justify constraining the distance to be greater than 0.15 assuming this measurement of color quality isn't a priority, resulting in Figure 21. With CS levels reaching close to 0.7 or full saturation with illuminance at 250 lx, it is worth exploring a tradeoff of color quality less similar to D65 for the gains in CS.

When using only pairs of emitters yielding a color distance of 0.15 and higher, we produce the model shown in Figures 21. We know that values can reach a distance of up

to 0.02 and still be within the D65 region so this last restriction is only appropriate for scenarios where white quality is less important. Therefore, recommendations for lighting from these latest emitter pairs can only be produced where standards don't require ANSI D65. The regression in Figure 21 will be discussed further in chapter V's future research section.

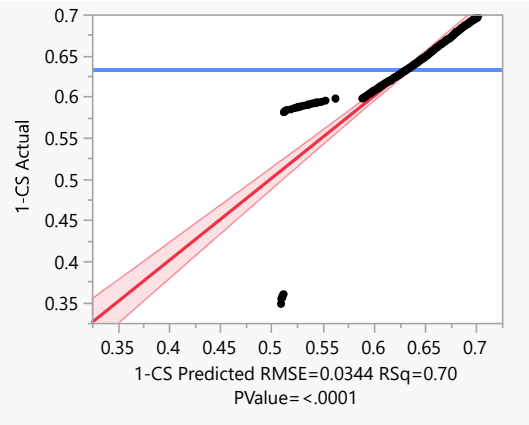

Figure 20: CS as predicted by color distance. Each point represents a selected emitter pair.

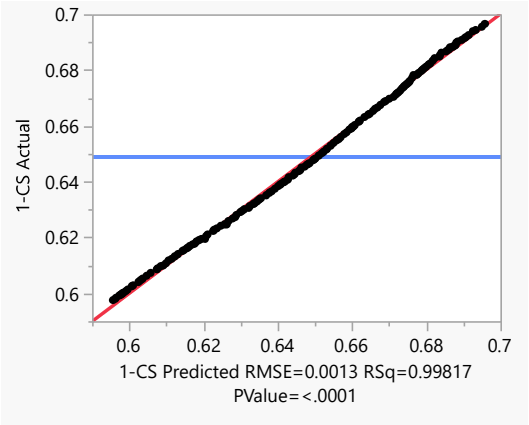

Figure 21: CS as predicted by color distance > 0.15. Each point represents a selected emitter pair.

The area of interest from Figure 19, where distance is close to 0.00 and CS values range from 0.43 to 0.58, are isolated and plotted in Figure 22. This plot includes color distance values that are outside the D65 region. We can see that CS values reach as high as 0.58 with a distance of 0.011. However, the associated CRI with this pair is -179 which is not a desirable value. This explains that high CRI values are achieved when the bandwidths are large as well as when the color is near D65. In this particular instance, we have identified that D65 is achieved, but the bandwidths are narrow.

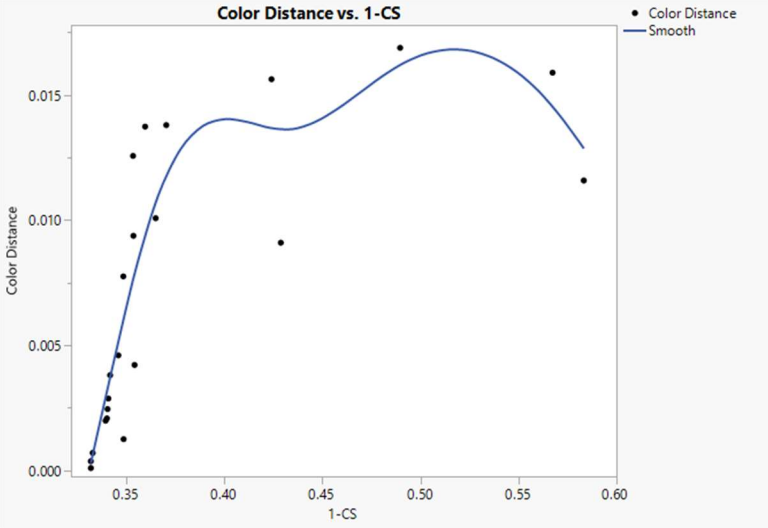

Figure 22: CS Predicted by Color Distance Close to or Within D65 Region. Each point represents an emitter pair.

Maximum CS Results

Finally, we assess the results of which emitter pairs maximize CS without any requirements for color. The values selected as the best overall will incorporate the corresponding properties of the wavelengths. We directed the genetic algorithm to list non-dominated emitter pair properties including centers, peaks, and widths in a matrix form displayed in Table 10. We see the best values of CS reach nearly full saturation of 0.7, with CRI values that are very low, indicating the color will appear more blue than white. This is typically undesirable. The blue peaks range from 380-405 nm with widths from 5-31 nm. The yellow peaks range from 705-760 with widths from 5-77 nm. The first three rows result in a very blue light since there is almost no yellow to balance the blue. We can see this because of how low the relative illuminance of the yellow peak is

compared to a blue illuminance of 1. Row four would result in magenta-colored lights as the center wavelength of the long wavelength emitter is nearer to red than yellow and the relative luminance of the long wavelength emitter is high. Selecting the emitter pairs among these with criteria solely based on maximum CS will yield either very blue or somewhat magenta colors.

Table 10: CS Without Color Parameters

Blue Peak	Blue Width	Yellow Peak	Yellow Width	Relative Illum	CS	CRI	Color Difference
380	5	760	5	0.0010	0.6993	-108.5410	0.3524
380	5	705	5	0.0010	0.6989	-101.6746	0.3518
380	5	760	77	0.0010	0.6977	-91.4153	0.3499
405	31	760	5	60.9848	0.6943	-81.6011	0.3498

Maximum CS with Constrained Color Results

This section assesses the emitter pairs which are selected to yield maximum values of CS with desirable color of light. In Table 11 we present the emitter pairs with additional criteria of maximum CS subject to a CRI > 70. The blue peaks range from 482-486 nm with widths from 99-115 nm. Yellow peaks stay constant at 760 nm again with widths from 174-190 nm. The maximum CS decreases from full saturation of 0.7 to 0.5195 when we constrain color. If we remember how much the widths of the blue and yellow emitters differed from Table 10, we can see here that the interval between the two shrinks, resulting in a much more balanced color of light, as we can see in the CRI values in column 7. The tradeoff here is that we still achieve the desirable CS > 0.3 while also obtaining a more acceptable color of light nearer D65.

Table 11: Non-Dominated Emitter Pairs CS Where CRI > 70

Blue Peak	Blue Width	Yellow Peak	Yellow Width	Relative Illum	CS	CRI	Color Difference
445	200	619	200	0.7822	0.3405	98.8594	0.0024
445	200	621	200	0.7822	0.3409	98.8284	0.0029
445	200	618	200	0.7822	0.3402	98.7649	0.0021
445	200	624	200	0.7822	0.3418	98.5577	0.0038
445	200	616	198	0.7822	0.3395	98.4691	0.0020
437	200	616	198	0.7822	0.3460	96.4764	0.0046
437	200	624	200	0.7822	0.3485	95.3526	0.0078
421	200	616	198	0.7822	0.3535	91.8197	0.0126
419	200	600	200	0.7822	0.3537	91.1018	0.0094
419	188	600	200	0.7822	0.3596	88.7770	0.0137
492	200	739	100	5.9384	0.3707	87.8650	0.0214
380	162	569	167	0.7671	0.3319	87.6879	0.0004
380	162	569	169	0.7671	0.3329	87.6723	0.0007
380	163	569	166	0.7671	0.3320	87.4591	0.0001
490	200	739	100	5.9384	0.3762	86.4869	0.0245
489	200	738	99	4.9384	0.3817	84.7057	0.0312
486	200	735	96	5.9384	0.3868	83.0736	0.0310
488	135	607	5	4.8603	0.3986	82.2073	0.0316
463	196	716	178	1.1729	0.3918	79.9347	0.0316
489	200	738	99	8.9384	0.3704	79.6818	0.0138
465	180	716	194	0.9229	0.4041	79.3220	0.0400
497	200	738	99	8.9384	0.3487	79.2745	0.0012
486	135	607	5	3.8603	0.4177	77.3910	0.0508
494	200	739	100	9.9384	0.3542	77.0393	0.0042
490	200	739	100	9.9384	0.3650	76.9994	0.0101
458	200	716	178	1.1729	0.3987	76.7414	0.0371
457	200	716	178	1.1729	0.3989	76.4835	0.0374
457	200	716	178	1.1729	0.3996	76.3643	0.0378
491	77	607	5	2.8603	0.4626	76.1570	0.0810
490	78	607	5	2.8603	0.4689	75.9751	0.0847
490	77	608	5	2.8603	0.4709	75.7992	0.0853
490	77	607	5	2.8603	0.4698	75.4917	0.0846
457	200	716	178	0.9854	0.4105	74.9394	0.0454
490	75	609	5	2.8603	0.4739	74.7484	0.0858
490	75	607	5	2.8603	0.4716	74.2236	0.0842
456	196	716	178	1.1729	0.4061	74.0552	0.0423
457	172	716	200	1.1729	0.4057	73.3518	0.0421
490	65	617	5	1.8603	0.5072	73.0121	0.1243
488	67	617	5	1.8603	0.5195	71.3287	0.1332
482	135	607	5	3.8603	0.4338	71.2661	0.0615
490	71	611	5	2.8603	0.4797	71.0847	0.0866
490	71	607	5	2.8603	0.4749	70.3664	0.0830
491	148	740	101	10.4384	0.3933	70.3011	0.0271

Thus far we have discussed the results we obtained when we only constrain the optimization of maximum CS and CRI. Earlier we mentioned we can obtain favorable CS

values of up to approximately 0.375 before distances begin to exit the boundaries of the D65 region. To better illustrate this optimization to minimize color difference we obtain the results shown in Table 12. When minimizing color difference, we are able to obtain very small distances certainly within the ANSI D65 specification, CRI's ranging from 79.27 to 87.68 and CS values from 0.3319 to 0.3487. This is the most interesting set of choices since the four lowest color differences also yields favorable values of CS and CRI.

Table 12: CS With Minimal Color Distance

Blue Peak	Blue Width	Yellow Peak	Yellow Width	Relative Illum	CS	CRI	Color Difference
380	163	569	166	0.7671	0.3320	87.4591	0.0001
380	162	569	167	0.7671	0.3319	87.6879	0.0004
380	162	569	169	0.7671	0.3329	87.6723	0.0007
497	200	738	99	8.9384	0.3487	79.2745	0.0012

Finally, we determine the optimal emitter pairs with respect to three different decision criteria displayed in Table 13. Maximizing CS produces full saturation near 0.7 with undesirable values for CRI of -108.5 and a color difference far from D65. Maximizing CRI produces a value near 99 and an acceptable CS of 0.34 and a color difference inside the D65 region. This is a useful set of choices, where all criteria are favorable. Finally, minimizing color difference gives us values near 0, which we saw in Table 12 with a CRI of 87.4 and a CS of 0.332. Using the optimal value of either color metric provides emitter pairs that yield favorable values.

Table 13: Optimal Value of Each Value Without Parameters

	Blue Peak	Blue Width	Yellow Peak	Yellow Width	Relative Illum	CS	CRI	Color Difference
Max CS	380	5	760	5	0	0.6993	-108.5410	0.3524
Max CRI	445	200	619	200	1	0.3405	98.8594	0.0024
Min Color Difference	380	163	569	166	1	0.3320	87.4591	0.0001

Since all values of CS when constraining for acceptable color measurements were greater than 0.3 it is a logical next step to provide the output for all emitter pairs that satisfy a CRI of greater than 70 and a color difference of less than or equal to 0.01. The output in Table 14 shows is that if we constrain color to be within the D65 region and also possess a CRI of greater than 70 we will obtain a CS of greater than 0.3

Table 14: CS When CRI > 70 and Color Distance is Within D65 Region

Blue Peak	Blue Width	Yellow Peak	Yellow Width	Relative Illum	CS	CRI	Color Difference
494	200	739	100	9.9384	0.3542	77.0393	0.0042
419	200	600	200	0.7822	0.3537	91.1018	0.0094
497	200	738	99	8.9384	0.3487	79.2745	0.0012
437	200	624	200	0.7822	0.3485	95.3526	0.0078
437	200	616	198	0.7822	0.3460	96.4764	0.0046
445	200	624	200	0.7822	0.3418	98.5577	0.0038
445	200	621	200	0.7822	0.3409	98.8284	0.0029
445	200	619	200	0.7822	0.3405	98.8594	0.0024
445	200	618	200	0.7822	0.3402	98.7649	0.0021
445	200	616	198	0.7822	0.3395	98.4691	0.0020
380	162	569	169	0.7671	0.3329	87.6723	0.0007
380	163	569	166	0.7671	0.3320	87.4591	0.0001
380	162	569	167	0.7671	0.3319	87.6879	0.0004

The final analyses in this work will provide the emitter pairs that produce the optimal values for CS, CRI, and color difference when holding luminance constant at 250 lx. Table 15 shows us that we can obtain a CS of 0.35 and also have CRI of 91 and a small color difference of 0.0094. The properties of this optimal emitter pair have a blue peak of 419 nm and blue width of 200 nm, a yellow peak of 600 nm and width of 200 nm

and a relative illuminance of 0.7822. A final note of importance for this optimal emitter pair is how broad the bandwidth is of these emitters. It may still be possible but this emphasizes that a greater number of emitters might be valuable as it is difficult to build emitters with a bandwidth this broad.

Table 15: Optimal Emitter Pair Selection

Blue Peak	Blue Width	Yellow Peak	Yellow Width	Relative Illum	CS	CRI	Color Difference
419	200	600	200	0.7822	0.3537	91.1018	0.0094

Summary

The information discussed in this chapter provided insight concerning the tradeoffs between CS, CRI, color difference, and relative efficacy. We perform multiple regression to develop baseline relationships between the considered variables. We then included requirements on colors to illustrate the different models that can be used where color and efficacy can be prioritized over CS in the form of a regression prediction equation. To better illustrate the tradeoffs, we perform a multi-objective analysis using a genetic algorithm to produce three pareto fronts. The first front includes CS, CRI, and color difference, and the second with CS and color difference, and the third with CS and CRI. The conclusions of analyses come in four sets; First, optimal predictors of CS using multiple regression, second, optimal emitter pairs with respect to maximum CS values without constraining color, third, optimal pairs with a CRI > 70, and fourth, the pareto front discussion of tradeoffs associated between two color metrics and CS. If we compare our results to those from the spectral data plotted in Figure 18 at 250 lx the loss in CS that

results from targeting a higher CRI and lesser color difference do not appear to be a significant limitation, since CS > 0.3 is still achieved.

The multiple regression model shown in Figure 15 (with the prediction formula in Equation (9)) models the dependent variable CS as a function of independent variables including the center wavelengths and widths of blue and yellow, and relative efficacy as independent variables. The emitter pair with the maximum CS value of 0.40, a CRI of 70.7, and relative efficacy of 0.47 is shown in Figure 15. It possesses a short wavelength emitter having a center wavelength of 480 nm with a bandwidth of 65 nm and a long wavelength emitter having a center wavelength of 595 nm and a bandwidth of 90 nm. The luminance output of the long wavelength emitter is 2.1 times the luminance output of the short wavelength emitter to achieve D65 as its color. The optimal emitter would have a blue emitter which is slightly longer in wavelength with a much broader emission than today's typical commercially available white LEDs.

Tables 6a, 7b, and 8c provides the values of maximum CS at 21.5 lx, 250 lx, and 500 lx without any requirements involving color. We concluded that without respect to color, illuminance and CS increase roughly linearly whereas color requirements and CS have an inverse relationship. Since we are concerned about illuminance levels and color, we incorporated color as an objective via a multi-objective genetic algorithm. The multidimensional pareto plot in Figures 5a and b are helpful in visualizing how color quality indeed does have an inverse relationship with CS values. From there it was useful to examine whether color difference or CRI were more useful in determining the CS of the emitter pair. Color difference led to a more linear fit when plotted against CS in Figure 19. Analyzing the non-dominated emitter pairs using only color difference and CS

we identified desirable CS values > 0.35 while remaining within the D65 region with an illuminance of 250 lx.

Considering constraints on CS, CRI, or color difference in isolation does not lead to favorable emitter pair selections in all objectives. However, constraining CRI to be greater than 70 and color difference to be less than 0.01 does provide thirteen useful emitter pairs, all providing a CS > 0.3. The final recommended emitter pair shown in Table 15 provides a CS = 0.3537 with a high CRI = 91, and a small color difference of 0.0094. Although the first row in Table 14 shows that there is a higher CS = 0.3542, and a color difference of 0.0042, the CRI = 77. Our conclusion is that a gain of 0.0005 in CS wasn't significant enough to justify a decrease from 91 to 77 in CRI.

V. Conclusions and Recommendations

Chapter Overview

Intelligence, Surveillance, & Reconnaissance (ISR) personnel among others performing sensitive operations are required to work in buildings without natural light. Further, many of these individuals perform shift work, requiring frequent changes in their work schedules. Research has shown that exposure to bright daylight suppresses the human body's production of melatonin, a hormone that regulates the sleep/wake cycle referred to as the circadian rhythm [10]. Research has also shown that some wavelengths of light are particularly useful for suppressing melatonin, especially in dim lighting environments [12]. The wavelengths that suppress the body's production of melatonin are found in most lighting fixtures, sunlight, and device screens. The human body produces more melatonin in dim or low light conditions resulting in increased sleepiness and decreased alertness [11]. Dim or no light is currently the regulatory state of lighting for many ISR work spaces, such as imagery analysts. In these environments, low light conditions enhance the visibility of low contrast objects on electronic displays. The results of this research have particular relevance for these environments.

Conclusions of Research

This thesis developed a model-based analysis and optimization approach to evaluate white light sources with two emitters in terms of circadian stimulus. Further, multiple regression analysis was used to focus attention on the characteristics of the spectrum that had the highest performance in terms of CS while providing useful color rendering as specified by CRI, distance from D65, and good luminance efficacy. The non-visual

effects of light are the focus of this regression analysis, with a goal of selecting light source characteristics that optimize the CS output with a constant target illuminance. The multiple regression model produces a prediction equation with a favorable adjusted R^2 = 0.764 and low RMSE = 0.0032 indicating that it represents CS relatively accurately for the range of light sources considered. Additionally, the associated p-values are sufficiently small (< 0.0001) to indicate the relationship between the dependent and independent variables is not a matter of chance. If these regression equations can be used to effectively represent 77%-90% (depending on CRI constraints) of the variation in CS accounted for by the independent variables, users can target desirable CS characteristics in two emitter light sources while maintaining adequate illuminance. This model was then used to assess the apparent trade-offs associated between CS, CRI, and color distance. This assessment leveraged a multi-objective procedure, producing a pareto front of non-dominated solutions in the complex multi-dimensional design space. This multi-objective approach leads to a simplified analysis focused on the most promising emitter combinations. The insights from this analysis indicate that the less we restrict color, the more gains there are to be made in CS while holding illuminance constant. This thesis demonstrates how this approach can be used to filter and select emitter combinations in a systematic and logical way. Based on the needs and regulations of a workspace, this approach can be used to prioritize CS and color to fit the needs of specific applications.

Significance of Research

This knowledge can be leveraged to educate lighting designers, managers, and individuals to target exposure of light in work centers and homes to promote enhanced

circadian rhythms. The case considered in this thesis research focused on two emitters within a single lamp which produces a range of CS values from about 0.16 to 0.44 at 250 lx. The optimal emitter pairs CS decreases to 0.35 when forcing color distance < 0.01, efficiency > 0.40 and CRI > 70. The results from this two-emitter analysis demonstrate the ability to improve the circadian stimulus by 20 percent above that available in existing lamps.

Recommendations for Action

The suggested recommendation begins with approaching lighting manufacturers to begin a dialog about the feasibility of constructing lamps which provide higher CS with lower illuminance, using this model to guide the exploration. Society continues to spend large amounts of time performing work and recreation indoors. The amount of time is increasing and the criticality of work performed in areas absent of any natural light is also increasing, especially in government related tasks. Policies and standards of light should be reexamined in depth to ensure the incorporation of regulations that consider the non-visual effects of light on human photoentrainment.

Recommendations for Future Research

Future research could explore how to utilize color difference measurements when considering more than two emitters. Additionally, one could attempt this same exercise utilizing a more perceptually uniform space such as u' v'. Using this space could provide more precise measurements involving an acceptable region of D65. It would also be interesting to incorporate the Melanopic Equivalent Daylight Illuminance (melEDI)

method of measuring the non-visual effects of light. The melEDI method assesses a light source by comparing it to daylight conditions [21]. A side-by-side comparison of the CS and the melEDI metrics and how they affect the light source design problem could be useful.

Levels of illuminance of 21.5 lx or less with the right conditions are often important in work areas. In this analysis, we found that CS > 0.3 cannot be achieved at 21.5 lx for light that is near D65 in color, but CS > 0.35 can be achieved at 250 lx. This analysis identifies significant tradeoffs involved in the emitter choices once CS is incorporated into the analysis. Substantial CS advantages can be achieved without compromising performance in visual tasks by considering this tradeoff carefully. However, more investigation is needed to gain a better understanding of the relationship between visual detection task performance and illuminance. As levels of illuminance increase from 21.5 lx, so will CS, and ultimately so will the human performance.

Summary

This research showed that modern lighting can be manipulated and leveraged to systematically consider the non-visual effects of light. Utilizing this model, the CS, CRI, and color difference of light can be optimized for suitability to the specific needs of the workplace or residential built environment. With the evidence that photoentrainment increases human performance and combats physical and mental health issues, any increase in CS from the existing conditions is significant. We found that if standards could allow for increases in illuminance and adjustments for trade-off with CRI and color difference, we can, in most cases, obtain a recommended CS > 0.3. Further research

should consider incorporating more emitters to explore higher gains in CS for increased synchronization of circadian systems.

Bibliography

[1] Kohl, Nathanael T., "The Influence of Light in the Built Environment to Improve Mental Health Outcomes" (2020). Theses and Dissertations. 4342. https://scholar.afit.edu/etd/4342

[2] Krantz, D. (2019, December 15). *Is blue light bad for you?* David Krantz - Epigenetic Health Coach. https://david-krantz.com/is-blue-light-bad-for-you/

[3] Leena Tähkämö, Timo Partonen & Anu-Katriina Pesonen (2019) Systematic review of light exposure impact on human circadian rhythm, Chronobiology International, 36:2, 151-170, DOI: 10.1080/07420528.2018.1527773

[4] Miller, Jeremy J., "Electronic Image Detectability under Varying Illumination Conditions" (2020). Theses and Dissertations. 3248. https://scholar.afit.edu/etd/3248

[5] Bolton, Sarah J., "Cognitive Effects of Short Duration Short Wavelength Visible Light" (2018). Theses and Dissertations. 1795. https://scholar.afit.edu/etd/1795

[6] Toh, K. L. (2008). Basic Science Review on Circadian Rhythm Biology and Circadian Sleep Disorders. *Annals Academy of Medicine*, *37*(8), 662-668. https://www.researchgate.net/profile/Kong-Toh/publication/23263932_Basic_science_review_on_circadian_rhythm_biology_and_circadian_sleep_disorders/links/5572ec7d08ae7536374e2635/Basic-science-review-on-circadian-rhythm-biology-and-circadian-sleep-disorders.pdf

[7] Dragoi, V. (2020, October 7). *Visual processing: Eye and retina (Section 2, Chapter 14) neuroscience online: An electronic textbook for the neurosciences | Department of Neurobiology and Anatomy - The University of Texas Medical School at Houston*. McGovern Medical School | Neurobiology & Anatomy. https://nba.uth.tmc.edu/neuroscience/m/s2/chapter14.html

[8] R. I. of Technology, “Rods & Cones.” [Online]. Available: https://www.cis.rit.edu/people/faculty/montag/vandplite/pages/chap_9/ch9p1.html.

[9] Hubel, D. H. (1995). *Eye, brain, and vision*. W. H. Freeman.

[10] Cajochen, C. (2020). Alerting effects of light. *Chronobiology*, *11*(27), 453-464. https://doi.org/10.1016/b978-3-437-21321-2.00004-1

[11] Sahin, L., Wood, B. M., Plitnick, B., & Figueiro, M. G. (2014). Daytime light exposure: Effects on biomarkers, measures of alertness, and performance. *Behavioural Brain Research*, *274*, 176-185. https://doi.org/10.1016/j.bbr.2014.08.017

[12] Badia, P., Myers, B., Boecker, M., Culpepper, J., & Harsh, J. (1991). Bright light effects on body temperature, alertness, EEG and behavior. *Physiology & Behavior*, *50*(3), 583-588. https://doi.org/10.1016/0031-9384(91)90549-4

[13] Graham, D. M., & Wong, K. Y. (2017). *Webvision: The organization of the retina and visual system*. Nature Publishing Group. https://webvision.med.utah.edu/book/part-ii-anatomy-and-physiology-of-the-retina/melanopsin-expressing-intrinsically-photosensitive-retinal-ganglion-cells/

[14] Matusiak, B., Kuhn, T., & Wirz-Justice, A. (2017). Sponsored collection | Changing perspectives on daylight: Science, technology, and culture. *Science*, *358*(6363), 680.2-680. https://doi.org/10.1126/science.358.6363.680-b

[15] Ryer, A. (1997). *Light measurement handbook*. International Light. http://www.chronobiology.ch/wp-content/uploads/publications/Cajochen_07.pdf

[16] Berthold Technologies, 2017. [Online]. Available: How to convert irradiance into photon flux - Berthold Technologies [Accessed: 03-March-2021].

[17] Gigahertz-Optik. (2021). *1.7 basic photometric quantities*. Lichtmesstechnik, Spektralradiometer und Ulbrichtkugeln. » Gigahertz-Optik. https://www.gigahertz-optik.com/en-us/basics-light-measurement/light-color/quantities-photometric

[18] NCAR. (2021). *Visible light*. UCAR Center for Science Education |. https://scied.ucar.edu/visible-light

[19] Honsberg, C., & Bowden, S. (n.d.). *Photon Flux*. PVEducation. https://www.pveducation.org/

[20] Figueiro, M., Kalsher, M., Steverson, B., Heerwagen, J., Kampschroer, K., & Rea, M. (2018). Circadian-effective light and its impact on alertness in office workers. *Lighting Research & Technology*, *51*(2), 171-183. https://doi.org/10.1177/1477153517750006

[21] Stefani, O., & Cajochen, C. (2021). Should we re-think regulations and standards for lighting at workplaces? A practice review on existing lighting recommendations. *Frontiers in Psychiatry*, *12*. https://doi.org/10.3389/fpsyt.2021.652161

[22] Pickard, G. E., & Sollars, P. J. (2011). Intrinsically photosensitive retinal ganglion cells. *Reviews of Physiology, Biochemistry and Pharmacology 162*, 59-90. https://doi.org/10.1007/112_2011_4

[23] Lighting Research Center (LRC). (n.d.). *How to Use the Look-Up Chart*. https://www.lrc.rpi.edu/programs/lighthealth/pdf/LookUpTable_Recessed-

Downlight.pdf. https://www.lrc.rpi.edu/programs/lighthealth/pdf/LookUpTable_Recessed-Downlight.pdf

[24] LRC. (2019, October 15). *Lighting research center videos on light and health | LRC research center* [Video]. LED Lighting, Lighting Design & Innovation | USAI Lighting. https://www.usailighting.com/lighting-research-center-videos-light-and-health

[25] Gennert, D. (2020, August 3). *How can you use light to set your sleep schedule?* The Rest - Eight Sleep. https://blog.eightsleep.com/light-sleep-schedule/

[26] Miller, M. E. (2018). *Color in electronic display systems: Advantages of multi-primary displays*. Springer.

[27] Miller, M., Gilman, J., & Colombi, J. (2014). A model for a two-source illuminant allowing daylight colour adjustment. *Lighting Research & Technology*, *48*(2), 239-252. https://doi.org/10.1177/1477153514559796

[28] Rea, M. S., Figueiro, M. G., Bullough, J. D., & Bierman, A. (2005). A model of phototransduction by the human circadian system. *Brain Research Reviews*, *50*(2), 213-228. https://doi.org/10.1016/j.brainresrev.2005.07.002

[29] Miller, M. E., & Shorter, P. (2016). 43-4: Revisiting lighting standards for critical viewing tasks. *SID Symposium Digest of Technical Papers*, *47*(1), 588-591. https://doi.org/10.1002/sdtp.10746

[30] Rensselaer Polytechnic Institute. (2020). *CS calculator*. Lighting Research Center. https://www.lrc.rpi.edu/cscalculator/

[31] Rea, M., & Figueiro, M. (2016). Light as a circadian stimulus for architectural lighting. *Lighting Research & Technology*, *50*(4), 497-510. https://doi.org/10.1177/1477153516682368

[32] National Center for Geospatial Intelligence Standards, "Softcopy Exploitation Standards." 2019.

[33] Lighting Research Center. (2020). *CS calculator*. https://www.lrc.rpi.edu/cscalculator/

REPORT DOCUMENTATION PAGE

Form Approved
OMB No. 074-0188

1. REPORT DATE *(DD-MM-YYYY)*	2. REPORT TYPE	3. DATES COVERED *(From – To)*
24-03-2022	Master's Thesis	September 2020 - March 2022

4. TITLE AND SUBTITLE
Applying Models of Circadian Stimulus to Explore Ideal Lighting Conditions

5a. CONTRACT NUMBER

5b. GRANT NUMBER

5c. PROGRAM ELEMENT NUMBER

6. AUTHOR(S)
Price, Alexander, J, MSgt

5d. PROJECT NUMBER
N/A

5e. TASK NUMBER

5f. WORK UNIT NUMBER

7. PERFORMING ORGANIZATION NAMES(S) AND ADDRESS(S)
Air Force Institute of Technology
Graduate School of Engineering and Management (AFIT/ENV)
2950 Hobson Way, Building 640
WPAFB OH 45433-8865

8. PERFORMING ORGANIZATION REPORT NUMBER
AFIT-ENS-MS-22-M-162

9. SPONSORING/MONITORING AGENCY NAME(S) AND ADDRESS(ES)
711 Human Performance Wing
Dr. Paul Havig
2255 H Street, Building 248
WPAFB OH 45433-8865
(937) 255-6655, paul.havig@us.af.mil ATTN: Dr. Paul Havig

10. SPONSOR/MONITOR'S ACRONYM(S)
711 HPW/RHWS

11. SPONSOR/MONITOR'S REPORT NUMBER(S)

12. DISTRIBUTION/AVAILABILITY STATEMENT
Distribution Statement A. Approved for public release; distribution unlimited.

13. SUPPLEMENTARY NOTES
This work is declared a work of the U.S. Government and is not subject to copyright protection in the United States.

14. ABSTRACT

Increased levels of time are spent indoors, decreasing human interaction with nature and degrading photoentrainment, the synchronization of circadian rhythms with daylight variation. Military imagery analysts, among other professionals, are required to work in low light level environments to limit power consumption or increase contrast on display screens to improve detail detection. Insufficient exposure to light in these environments results in inadequate photoentrainment which is associated with degraded alertness and negative health effects. Recent research has shown that both the illuminance (i.e., perceived intensity) and wavelength of light affect photoentrainment. Simultaneously, modern lighting technologies have improved our ability to construct lights with desired wavelengths. To improve photoentrainment in low light environments, this research utilizes a multiple regression and multi-objective model to explore the relationship between the wavelength composition of artificial light and circadian stimulus (CS) for a fixed illuminance. The model is used to recommend emitter light intensity and wavelength characteristics that maximize CS in artificial lighting. These results suggest that by carefully choosing the center wavelengths for emitters we can achieve desirable CS values without increasing intensity. In addition, constraining the design to low illuminance values leads to increases in blue wavelength energy and shifts the color of illumination. Finally, constraining the design to a desirable range of colors reduces the size of this effect while still providing desirable levels of CS. The highest CS achieved at 250 lx is 0.669 without consideration for CRI or color difference. Constraining CRI and color to match D65, the maximum CS at 250 lx is 0.353 with a CRI of 91.1 and a color difference from D65 of 0.0094.

15. SUBJECT TERMS
Lighting, Illumination, Alertness, Multiple Regression Models, Multi-objective Optimization

16. SECURITY CLASSIFICATION OF:			17. LIMITATION OF ABSTRACT	18. NUMBER OF PAGES	19a. NAME OF RESPONSIBLE PERSON
a. REPORT	b. ABSTRACT	c. THIS PAGE			Dr. Michael E. Miller AFIT/ENV
U	U	U	UU	92	19b. TELEPHONE NUMBER *(Include area code)* (937) 255-6565, x 4625 (Michael.Miller@afit.edu)